Neutralino decay of MSSM neutral Higgs bosons

Tarek Ibrahim

Department of Physics, Faculty of Science, Alexandria University, Egypt
and
Department of Physics, Northeastern University, Boston, MA 02115-5000, USA [1]

Abstract

We compute the one loop corrected effective Lagrangian for the neutralino-neutralino-neutral Higgs interactions $\chi^0_\ell \chi^0_k H^0_m$. The analysis completes the previous analyses where similar corrections were computed for the $\bar{f} f H^0_m$ couplings, where f stands for Standard Model quarks and leptons and for the chargino-chargino-neutral Higgs couplings $\chi^+_l \chi^-_k H^0_m$ within the minimal supersymmetric standard model MSSM. The effective one loop Lagrangian is then applied to the computation of the neutral Higgs decays. The sizes of the supersymmetric loop corrections of the neutral Higgs decay widths into $\chi^0_\ell \chi^0_k$ ($\ell = 1,2,3,4$; $k = 1,2,3,4$) are investigated and the supersymmetric loop correction is found to be in the range of $\sim 10\%$ in significant regions of the parameter space. By including the loop corrections of the other decay channels $\bar{b}b$, $\bar{t}t$, $\bar{\tau}\tau$, $\bar{c}c$, and $\chi^-_i \chi^+_j$ ($i = 1,2$; $j = 1,2$), the corrections to branching ratios for $H^0_m \to \chi^0_\ell \chi^0_k$ can reach as high as 50%. The effects of CP phases on the branching ratio are also investigated. A discussion of the implications of the analysis for colliders is given.

[1] Current address

1 INTRODUCTION

The Higgs couplings to matter and gauge fields are of current interest as they affect different phenomena which could be tested in low energy processes [1]. Recently calculations of the supersymmetric one loop corrections to the Higgs boson couplings were given and their implications for the neutral Higgs boson decays into $\bar{b}b$, $\bar{t}t$, $\bar{\tau}\tau$, $\bar{c}c$ and $\chi_i^- \chi_j^+$ were analyzed [2]. These decays are of great importance as they differ from the Higgs decay predictions in the Higgs sector of the standard model. In this work we extend the analysis to include the loop corrections of the $\chi_\ell^0 \chi_k^0 H_m^0$ couplings and the neutral Higgs decay into pairs of neutralinos. The complete analysis of the one loop corrected partial widths of the above channels allows one to investigate also the effects of these corrections on the branching ratios of different modes.

In this paper we include the effect of CP phases arising from the soft supersymmetric breaking parameters. It is well known that large CP phases would induce electric dipole moments of the fermions in the theory. However these large CP phases can be made compatible [3, 4, 5] with the severe experimental constraints that exist on the electric dipole moments of the electron [6], of the neutron [7], and of the Hg^{199} [8]. It is well known that if the phases are large they affect a variety of low energy phenomena [9]. Some works in this direction have included the effects of CP phases on the neutral Higgs boson system. These phases induce mixings between the neutral CP even and the CP odd Higgs and can affect the decay of the neutral and charged Higgs into different modes [10].

The current analysis of $\Delta\mathcal{L}_{\chi^0\chi^0 H^0}$ and neutral Higgs decay into neutralinos is based on the effective Lagrangian method where the couplings of the electroweak eigen states H_1^1 and H_2^2 with neutralinos are radiatively corrected using the zero external momentum approximation. The same technique has been used in calculating the effective Lagrangian and decays of H_m^0 into quarks and leptons [1, 11, 12] and into chargino pairs [2]. It has been used also in the analysis of the effective Lagrangian of charged Higgs with quarks [1, 13] and their decays into $\bar{t}b$ and $\nu_\tau\tau$ [14] and into chargino + neutralino [15]. The neutral Higgs decays into neutralinos have been investigated before in the CP conserving case [16, 17]. However, the analysis for the neutral Higgs decays into neutralinos, with one loop corrections, in the CP violating case where the neutral Higgs sector is modified in couplings, spectrum and mixings, does not exist. We evaluate the radiative corrections to the Higgs boson masses and mixngs by using the effective potential approximation.

We include the corrections from the top and bottom quarks and squarks [18], from the chargino, the W and the charged Higgs sector [19] and from the neutralino, Z boson, and the neutral Higgs bosons [20]. It is important to notice that the corrections to the Higgs effective potential from the different sectors mentioned above are all one-loop corrections. The corrections of the interaction $\Delta\mathcal{L}_{\chi^0\chi^0 H^0}$ to be considered in this work are all one-loop level ones. So the analysis presented here is a consistent one loop study.

The outline of the rest of the paper is as follows: In Sec. 2 we compute the effective Lagrangian for the $\chi^0_\ell\chi^0_k H^0_m$ interaction. In Sec. 3 we give an analysis of the decay widths of the neutral Higgs bosons into neutralinos using the effective Lagrangian. In Sec. 4 we give a numerical analysis of the size of the loop effects on the partial decay widths and on the branching ratios. In Sec. 5 we discuss the implications of the corrections considered here, in the environment of the Large Hadron Collider LHC. Conclusions are given in Sec. 6.

2 LOOP CORRECTIONS TO NEUTRAL HIGGS COUPLINGS

The tree-level Lagrangian for $\chi^0_\ell\chi^0_k H^0$ interaction is

$$\mathcal{L} = \theta_{k\ell}\overline{\chi^0_k}P_L\chi^0_\ell H^{1*}_1 + \tau_{k\ell}\overline{\chi^0_k}P_R\chi^0_\ell H^2_2 + H.c., \tag{1}$$

where H^1_1 and H^2_2 are the neutral states of the two Higgs isodoublets in the minimal supersymmetric standard model (MSSM), i.e.,

$$(H_1) = \begin{pmatrix} H^1_1 \\ H^2_1 \end{pmatrix}, \quad (H_2) = \begin{pmatrix} H^1_2 \\ H^2_2 \end{pmatrix} \tag{2}$$

and $\theta_{k\ell} = -gQ^{*'}_{k\ell}$ and $\tau_{k\ell} = gS'_{\ell k}$ where

$$Q'_{ij} = \frac{1}{\sqrt{2}}[X^*_{3i}(X^*_{2j} - \tan\theta_W X^*_{1j})] \tag{3}$$

$$S'_{ij} = \frac{1}{\sqrt{2}}[X^*_{4j}(X^*_{2i} - \tan\theta_W X^*_{1i})] \tag{4}$$

The matrix elements X are defined as

$$X^T M_{\chi^0} X = diag(m_{\chi^0_1}, m_{\chi^0_2}, m_{\chi^0_3}, m_{\chi^0_4}) \tag{5}$$

where M_{χ^0} is the 4×4 neutralino mass matrix.

The loop corrections produce shifts in the couplings of Eq. (1) and the effective Lagrangian with loop corrected couplings is given by

$$\mathcal{L}_{eff} = (\theta_{k\ell} + \delta\theta_{k\ell})\overline{\chi_k^0} P_L \chi_\ell^0 H_1^{1*} + \Delta\theta_{k\ell}\overline{\chi_k^0} P_L \chi_\ell^0 H_2^2 + (\tau_{k\ell} + \delta\tau_{k\ell})\overline{\chi_k^0} P_R \chi_\ell^0 H_2^2 + \Delta\tau_{k\ell}\overline{\chi_k^0} P_R \chi_\ell^0 H_1^{1*} + H.c. \tag{6}$$

In this work we calculate the loop corrections $\delta\theta_{k\ell}$, $\Delta\tau_{k\ell}$, $\Delta\theta_{k\ell}$ and $\delta\tau_{k\ell}$ using the zero external momentum approximation.

2.1 Loop analysis of $\delta\theta_{k\ell}$ and $\Delta\tau_{k\ell}$

Contributions to $\delta\theta_{k\ell}$ and $\Delta\tau_{k\ell}$ arise from the fourteen loop diagram of Fig. 1. We discuss now in detail the contribution of each of these diagrams. The basic integral that enters in the loop analysis is

$$J = \int \frac{d^4\ell}{(2\pi)^4} \frac{1}{(\ell^2 - m_1^2 + i\epsilon)(\ell^2 - m_2^2 + i\epsilon)(\ell^2 - m_3^2 + i\epsilon)} \tag{7}$$

where m_1, m_2 and m_3 are the masses of the particles running inside the loops. This integral gives

$$J = \frac{i}{(4\pi)^2} f(m_1^2, m_2^2, m_3^2) \tag{8}$$

where

$$f(m_1^2, m_2^2, m_3^2) = \frac{1}{(m_1^2 - m_3^2)} \frac{1}{(m_3^2 - m_2^2)} \frac{1}{(m_1^2 - m_2^2)} \times [m_2^2 m_3^2 \ln(\frac{m_2^2}{m_3^2}) + m_3^2 m_1^2 \ln(\frac{m_3^2}{m_1^2}) + m_1^2 m_2^2 \ln(\frac{m_1^2}{m_2^2})] \tag{9}$$

and for the case of $m_2 = m_3$, one finds

$$J = \frac{i}{(4\pi)^2} \frac{1}{(m_3^2 - m_1^2)^2} [m_1^2 \ln(\frac{m_3^2}{m_1^2}) + m_1^2 - m_3^2] \tag{10}$$

We begin with the loop diagram of Fig. 1(i), part (a), which contributes the following to $\delta\theta_{k\ell}$ and $\Delta\tau_{k\ell}$:

$$\begin{aligned} \delta\theta_{k\ell}^{(1)} &= -\sum_{i=1}^{2}\sum_{j=1}^{2} \frac{m_t}{8\pi^2} F_{ji}^* (\alpha_{t\ell} D_{t1j} - \gamma_{t\ell} D_{t2j}) \\ &\quad \times (\beta_{tk}^* D_{t1i}^* + \alpha_{tk} D_{t2i}^*) f(m_t^2, m_{\tilde{t}_i}^2, m_{\tilde{t}_j}^2) \\ \Delta\tau_{k\ell}^{(1)} &= -\sum_{i=1}^{2}\sum_{j=1}^{2} \frac{m_t}{8\pi^2} F_{ji}^* (\beta_{t\ell} D_{t1j} + \alpha_{t\ell}^* D_{t2j}) \\ &\quad \times (\alpha_{tk}^* D_{t1i}^* - \gamma_{tk}^* D_{t2i}^*) f(m_t^2, m_{\tilde{t}_i}^2, m_{\tilde{t}_j}^2) \end{aligned} \tag{11}$$

where F_{ji} is given by

$$F_{ji} = -\frac{gM_Z}{\sqrt{2}\cos\theta_W}((\frac{1}{2} - \frac{2}{3}\sin^2\theta_W)D^*_{t1j}D_{t1i} + \frac{2}{3}\sin^2\theta_W D^*_{t2j}D_{t2i})\cos\beta + \frac{gm_t\mu}{\sqrt{2}m_W\sin\beta}D^*_{t1j}D_{t2i} \quad (12)$$

The couplings α_{tk}, β_{tk} and γ_{tk} are given by

$$\alpha_{tk} = \frac{gm_tX_{4k}}{2m_W\sin\beta}$$
$$\beta_{tk} = eQ_tX'^*_{1k} + \frac{g}{\cos\theta_W}X'^*_{2k}(T_{3t} - Q_t\sin^2\theta_W)$$
$$\gamma_{tk} = eQ_tX'_{1k} - \frac{gQ_t\sin^2\theta_W}{\cos\theta_W}X'_{2k} \quad (13)$$

where X''s are given by

$$X'_{1k} = X_{1k}\cos\theta_W + X_{2k}\sin\theta_W$$
$$X'_{2k} = -X_{1k}\sin\theta_W + X_{2k}\cos\theta_W \quad (14)$$

The matrix elements D_q are diagonalizing the squark mass^2 matrix as follows

$$D_q^+M^2_{\tilde{q}}D_q = diag(m^2_{\tilde{q}1}, m^2_{\tilde{q}2}) \quad (15)$$

Next for the loop Fig. 1(i), part(b), we find

$$\delta\theta^{(2)}_{k\ell} = -\sum_{i=1}^{2}\sum_{j=1}^{2}\frac{m_b}{8\pi^2}H^*_{ij}(\alpha_{b\ell}D_{b1j} - \gamma_{b\ell}D_{b2j}) \times(\beta^*_{bk}D^*_{b1i} + \alpha_{bk}D^*_{b2i})f(m^2_b, m^2_{\tilde{b}_i}, m^2_{\tilde{b}_j})$$
$$\Delta\tau^{(2)}_{k\ell} = -\sum_{i=1}^{2}\sum_{j=1}^{2}\frac{m_b}{8\pi^2}H^*_{ij}(\beta_{b\ell}D_{b1j} + \alpha^*_{b\ell}D_{b2j}) \times(\alpha^*_{bk}D^*_{b1i} - \gamma^*_{bk}D^*_{b2i})f(m^2_b, m^2_{\tilde{b}_i}, m^2_{\tilde{b}_j}) \quad (16)$$

and H_{ij} is given by

$$H_{ij} = -\frac{gM_Z}{\sqrt{2}\cos\theta_W}((-\frac{1}{2} + \frac{1}{3}\sin^2\theta_W)D^*_{b1i}D_{b1j} - \frac{1}{3}\sin^2\theta_W D^*_{b2i}D_{b2j})\cos\beta - \frac{gm_b^2}{\sqrt{2}m_W\cos\beta}(D^*_{b1i}D_{b1j} + D^*_{b2i}D_{b2j}) - \frac{gm_bA_b}{\sqrt{2}m_W\cos\beta}D^*_{b2i}D_{b1j} \quad (17)$$

For the loop of Fig. 1(ii), part(a), we find

$$\delta\theta^{(3)}_{k\ell} = 0$$
$$\Delta\tau^{(3)}_{k\ell} = 0 \quad (18)$$

For the loop of Fig. 1(ii), part(b), we find

$$\begin{aligned}\delta\theta^{(4)}_{k\ell} &= 0\\ \Delta\tau^{(4)}_{k\ell} &= \sum_{j=1}^{2}\frac{h_b m_b^2}{8\pi^2}(\beta_{b\ell}D_{b1j}+\alpha^*_{b\ell}D_{b2j})\\ &\times(\alpha^*_{bk}D^*_{b1j}-\gamma^*_{bk}D^*_{b2j})f(m^2_{\tilde{b}_j},m_b^2,m_b^2)\end{aligned} \tag{19}$$

where h_b is given by

$$h_b = \frac{g m_b}{\sqrt{2}m_W\cos\beta} \tag{20}$$

For loop of Fig. 1(ii), part(c), we find

$$\begin{aligned}\delta\theta^{(5)}_{k\ell} &= -\sum_{i=1}^{4}\sum_{j=1}^{4}\frac{g^3}{2\pi^2\cos^2\theta_W}Q'^*_{ij}R'''_{kj}L'''_{i\ell}\\ &\times m_{\chi^0_i}m_{\chi^0_j}f(m^2_{\chi^0_i},m^2_{\chi^0_j},m_Z^2)\\ \Delta\tau^{(5)}_{k\ell} &= 0\end{aligned} \tag{21}$$

where the couplings L'''_{ij} and R'''_{ij} are given by

$$L'''_{ij} = -R'''^*_{ij} = -\frac{1}{2}X^*_{3i}X_{3j}+\frac{1}{2}X^*_{4i}X_{4j} \tag{22}$$

For loop of Fig. 1(ii), part(d), we find

$$\begin{aligned}\delta\theta^{(6)}_{k\ell} &= \sum_{i=1}^{4}\sum_{j=1}^{4}\sum_{n=1}^{3}\frac{g^3}{4\pi^2}Q'^*_{ij}\\ &\{Q'^*_{i\ell}(Y_{n1}-iY_{n3}\sin\beta)-S'^*_{i\ell}(Y_{n2}-iY_{n3}\cos\beta)\}\\ &\times\{Q'^*_{kj}(Y_{n1}-iY_{n3}\sin\beta)-S'^*_{kj}(Y_{n2}-iY_{n3}\cos\beta)\}\\ &m_{\chi^0_i}m_{\chi^0_j}f(m^2_{\chi^0_i},m^2_{\chi^0_j},m^2_{H^0_n})\\ \Delta\tau^{(6)}_{k\ell} &= 0\end{aligned} \tag{23}$$

where the matrix elements Y are diagonalizing the neutral Higgs mass^2 matrix as follows $YM^2_{Higgs}Y^T = diag(m^2_{H^0_1},m^2_{H^0_2},m^2_{H^0_3})$.

For loop of Fig. 1(i), part(c), we find

$$\begin{aligned}\delta\theta^{(7)}_{k\ell} = \frac{g^3 m_Z\cos\beta}{4\sqrt{2}\cos\theta_W}\sum_{i=1}^{4}\sum_{n=1}^{3}\sum_{m=1}^{3}&\{Q'^*_{i\ell}(Y_{n1}-iY_{n3}\sin\beta)-S'^*_{i\ell}(Y_{n2}-iY_{n3}\cos\beta)\}\\ &\{Q'^*_{ki}(Y_{m1}-iY_{m3}\sin\beta)-S'^*_{ki}(Y_{m2}-iY_{m3}\cos\beta)\}\\ &\{(Y_{n1}+iY_{n3}\sin\beta)(3Y_{m1}-iY_{m3}\sin\beta-4Y_{m2}\tan\beta)\end{aligned}$$

$$-2(Y_{m2}-iY_{m3}\cos\beta)(Y_{n2}+iY_{n3}\cos\beta)\}\frac{m_{\chi_i^0}}{16\pi^2}f(m^2_{\chi_i^0},m^2_{H_m^0},m^2_{H_n^0})$$

$$\Delta\tau_{k\ell}^{(7)}=\frac{g^3m_Z\cos\beta}{4\sqrt{2}\cos\theta_W}\sum_{i=1}^{4}\sum_{n=1}^{3}\sum_{m=1}^{3}\{Q'_{\ell i}(Y_{n1}+iY_{n3}\sin\beta)-S'_{\ell i}(Y_{n2}+iY_{n3}\cos\beta)\}$$
$$\{Q'_{ik}(Y_{m1}+iY_{m3}\sin\beta)-S'_{ik}(Y_{m2}+iY_{m3}\cos\beta)\}$$
$$\{(Y_{n1}+iY_{n3}\sin\beta)(3Y_{m1}-iY_{m3}\sin\beta-4Y_{m2}\tan\beta)$$
$$-2(Y_{m2}-iY_{m3}\cos\beta)(Y_{n2}+iY_{n3}\cos\beta)\}\frac{m_{\chi_i^0}}{16\pi^2}f(m^2_{\chi_i^0},m^2_{H_m^0},m^2_{H_n^0}) \quad (24)$$

For loop of Fig. 1(i), part(d), we find

$$\delta\theta_{k\ell}^{(8)}=-\frac{2g^3m_Z\cos\beta}{\sqrt{2}\cos^3\theta_W}\sum_{i=1}^{4}R'''_{ki}L'''_{i\ell}\frac{m_{\chi_i^0}}{16\pi^2}f(m^2_{\chi_i^0},m^2_Z,m^2_Z)$$
$$\Delta\tau_{k\ell}^{(8)}=-\frac{2g^3m_Z\cos\beta}{\sqrt{2}\cos^3\theta_W}\sum_{i=1}^{4}L'''_{ki}R'''_{i\ell}\frac{m_{\chi_i^0}}{16\pi^2}f(m^2_{\chi_i^0},m^2_Z,m^2_Z) \quad (25)$$

For loop of Fig. 1(ii), part(e), we find

$$\delta\theta_{k\ell}^{(9)}=-\sum_{i=1}^{2}\sum_{j=1}^{2}\epsilon_{kj}\epsilon'^{*}_{\ell i}\phi^*_{ij}\cos\beta\sin\beta$$
$$\frac{m_{\chi_i^+}m_{\chi_j^+}}{16\pi^2}f(m^2_{\chi_i^+},m^2_{\chi_j^+},m^2_{H^-})$$
$$\Delta\tau_{k\ell}^{(9)}=0 \quad (26)$$

The parameters ϵ_{ij}, ϵ'_{ij} and ϕ_{ij} are defined by

$$\epsilon_{ij}=-gX_{4i}V^*_{j1}-\frac{g}{\sqrt{2}}X_{2i}V^*_{j2}-\frac{g}{\sqrt{2}}\tan\theta_WX_{1i}V^*_{j2}$$
$$\epsilon'_{ij}=-gX^*_{3i}U_{j1}+\frac{g}{\sqrt{2}}X^*_{2i}U_{j2}+\frac{g}{\sqrt{2}}\tan\theta_WX^*_{1i}U_{j2}$$
$$\phi_{ij}=-gU_{j2}V_{i1} \quad (27)$$

where the diagonalizing matrices U and V of the chargino mass matrix are defined by

$$U^*M_{\chi^+}V^{-1}=diag(m_{\chi_1^+},m_{\chi_2^+}) \quad (28)$$

For loop of Fig. 1(i), part(e), we find

$$\delta\theta_{k\ell}^{(10)}=\frac{gm_W}{2\sqrt{2}}\sum_{i=1}^{2}\epsilon_{ki}\epsilon'^{*}_{\ell i}\cos^2\beta\sin\beta(1+2\sin^2\beta-\cos2\beta\tan^2\theta_W)$$
$$\times\frac{m_{\chi_i^+}}{16\pi^2}f(m^2_{\chi_i^+},m^2_{H^-},m^2_{H^-})$$
$$\Delta\tau_{k\ell}^{(10)}=\frac{gm_W}{2\sqrt{2}}\sum_{i=1}^{2}\epsilon'_{ki}\epsilon^*_{\ell i}\cos^2\beta\sin\beta(1+2\sin^2\beta-\cos2\beta\tan^2\theta_W)$$
$$\times\frac{m_{\chi_i^+}}{16\pi^2}f(m^2_{\chi_i^+},m^2_{H^-},m^2_{H^-}) \quad (29)$$

For loop of Fig. 1(i), part(f), we find

$$\delta\theta^{(11)}_{k\ell} = -\sum_{i=1}^{2}\frac{g^3}{\sqrt{2}}m_W\cos\beta R_{ki}L^*_{\ell i}\frac{m_{\chi_i^+}}{4\pi^2}f(m^2_{\chi_i^+},m^2_{W^-},m^2_{W^-})$$
$$\Delta\tau^{(11)}_{k\ell} = -\sum_{i=1}^{2}\frac{g^3}{\sqrt{2}}m_W\cos\beta R^*_{\ell i}L_{ki}\frac{m_{\chi_i^+}}{4\pi^2}f(m^2_{\chi_i^+},m^2_{W^-},m^2_{W^-}) \quad (30)$$

where L and$R$ are defined as

$$L_{ij} = -\frac{1}{\sqrt{2}}X^*_{4i}V^*_{j2} + X^*_{2i}V^*_{j1}$$
$$R_{ij} = \frac{1}{\sqrt{2}}X_{3i}U_{j2} + X_{2i}U_{j1} \quad (31)$$

For loop of Fig. 1(ii), part(f), we find

$$\delta\theta^{(12)}_{k\ell} = 0$$
$$\Delta\tau^{(12)}_{k\ell} = \sum_{i=1}^{2}\sum_{j=1}^{2}g^2\phi^*_{ij}L_{kj}R^*_{\ell i}\frac{m_{\chi_i^+}m_{\chi_j^+}}{4\pi^2}f(m^2_{\chi_i^+},m^2_{\chi_j^+},m^2_{W^-}) \quad (32)$$

For loop of Fig. 1(ii), part(g), we find

$$\delta\theta^{(13)}_{k\ell} = 0$$
$$\Delta\tau^{(13)}_{k\ell} = \sum_{i=1}^{2}\frac{h_\tau m_\tau^2}{8\pi^2}(\beta_{\tau\ell}D_{\tau 1i} + \alpha^*_{\tau\ell}D_{\tau 2i})$$
$$\times(\alpha^*_{\tau k}D^*_{\tau 1i} - \gamma^*_{\tau k}D^*_{\tau 2i})f(m^2_{\tilde{\tau}_i},m^2_\tau,m^2_\tau) \quad (33)$$

where

$$h_\tau = \frac{gm_\tau}{\sqrt{2}m_W\cos\beta} \quad (34)$$

For loop of Fig. 1(i), part(g), we find

$$\delta\theta^{(14)}_{k\ell} = -\sum_{i=1}^{2}\sum_{j=1}^{2}\frac{m_\tau}{8\pi^2}H^*_{\tau ji}(\alpha_{\tau\ell}D_{\tau 1i} - \gamma_{\tau\ell}D_{\tau 2i})$$
$$\times(\beta^*_{\tau k}D^*_{\tau 1i} + \alpha_{\tau k}D^*_{\tau 2j})f(m^2_\tau,m^2_{\tilde{\tau}_i},m^2_{\tilde{\tau}_j})$$
$$\Delta\tau^{(14)}_{k\ell} = -\sum_{i=1}^{2}\sum_{j=1}^{2}\frac{m_\tau}{8\pi^2}H^*_{\tau ji}(\beta_{\tau\ell}D_{\tau 1i} + \alpha^*_{\tau\ell}D_{\tau 2i})$$
$$\times(\alpha^*_{\tau k}D^*_{\tau 1j} - \gamma^*_{\tau k}D^*_{\tau 2j})f(m^2_\tau,m^2_{\tilde{\tau}_i},m^2_{\tilde{\tau}_j}) \quad (35)$$

and $H_{\tau ij}$ is given by

$$H_{\tau ij} = -\frac{gM_Z}{\sqrt{2}\cos\theta_W}((-\frac{1}{2}+\sin^2\theta_W)D^*_{\tau 1i}D_{\tau 1j} - \sin^2\theta_W D^*_{\tau 2i}D_{\tau 2j})\cos\beta$$
$$-\frac{gm_\tau^2}{\sqrt{2}m_W\cos\beta}(D^*_{\tau 1i}D_{\tau 1j} + D^*_{\tau 2i}D_{\tau 2j}) - \frac{gm_\tau A_\tau}{\sqrt{2}m_W\cos\beta}D^*_{\tau 2i}D_{\tau 1j} \quad (36)$$

The loop corrections for $\delta\theta_{k\ell}$ and $\Delta\tau_{k\ell}$ are given by

$$\delta\theta_{k\ell} = \sum_{n=1}^{14} \delta\theta_{k\ell}^{(n)}$$
$$\Delta\tau_{k\ell} = \sum_{n=1}^{14} \Delta\tau_{k\ell}^{(n)} \tag{37}$$

2.2 Loop analysis of $\Delta\theta_{k\ell}$ and $\delta\tau_{k\ell}$

We do the same analysis of Figure 2 as for Figure 1. We write down here the final results for both corrections from the fourteen loops together. The corrections are written in the same order of the loops in Figure 2.

$$\begin{aligned}
\Delta\theta_{k\ell} = &-\sum_{i=1}^{2}\sum_{j=1}^{2}\frac{m_t}{8\pi^2}E_{ji}(\alpha_{t\ell}D_{t1j}-\gamma_{t\ell}D_{t2j})(\beta^*_{tk}D^*_{t1i}+\alpha_{tk}D^*_{t2i})f(m_t^2,m^2_{\tilde{t}_i},m^2_{\tilde{t}_j})\\
&-\sum_{i=1}^{2}\sum_{j=1}^{2}\frac{m_b}{8\pi^2}G_{ji}(\alpha_{b\ell}D_{b1j}-\gamma_{b\ell}D_{b2j})(\beta^*_{bk}D^*_{b1i}+\alpha_{bk}D^*_{b2i})f(m_b^2,m^2_{\tilde{b}_i},m^2_{\tilde{b}_j})\\
&+\sum_{j=1}^{2}\frac{m_t^2h_t}{8\pi^2}(\alpha_{t\ell}D_{t1j}-\gamma_{t\ell}D_{t2j})(\beta^*_{tk}D^*_{t1j}+\alpha_{tk}D^*_{t2j})f(m^2_{\tilde{t}_j},m_t^2,m_t^2)\\
&+0\\
&+0\\
&+0\\
&+\frac{g^3m_Z\cos\beta}{4\sqrt{2}\cos\theta_W}\sum_{i=1}^{4}\sum_{n=1}^{3}\sum_{m=1}^{3}\{Q'^*_{i\ell}(Y_{n1}-iY_{n3}\sin\beta)-S'^*_{i\ell}(Y_{n2}-iY_{n3}\cos\beta)\}\\
&\{Q'^*_{ki}(Y_{m1}-iY_{m3}\sin\beta)-S'^*_{ki}(Y_{m2}-iY_{m3}\cos\beta)\}\{\tan\beta(Y_{n2}-iY_{n3}\cos\beta)(3Y_{m2}+iY_{m3}\cos\beta)\\
&-4Y_{n1}(Y_{m2}-iY_{m3}\cos\beta)-2\tan\beta(Y_{m1}-iY_{m3}\sin\beta)(Y_{n1}+iY_{n3}\sin\beta)\}\frac{m_{\chi_i^0}}{16\pi^2}f(m^2_{\chi_i^0},m^2_{H_m^0},m^2_{H_n^0})\\
&-\frac{2g^3m_Z\sin\beta}{\sqrt{2}\cos^3\theta_W}\sum_{i=1}^{4}R'''_{ki}L'''_{i\ell}\frac{m_{\chi_i^0}}{16\pi^2}f(m^2_{\chi_i^0},m_Z^2,m_Z^2)\\
&+0\\
&+\frac{gm_W}{2\sqrt{2}}\sum_{i=1}^{2}\epsilon_{ki}\epsilon'^*_{\ell i}\cos\beta\sin^2\beta(1+2\cos^2\beta+\cos2\beta\tan^2\theta_W)\frac{m_{\chi_i^+}}{16\pi^2}f(m^2_{\chi_i^+},m^2_{H^-},m^2_{H^-})\\
&-\sum_{i=1}^{2}\frac{g^3}{\sqrt{2}}m_W\sin\beta R_{ki}L^*_{\ell i}\frac{m_{\chi_i^+}}{4\pi^2}f(m^2_{\chi_i^+},m^2_{W^-},m^2_{W^-})\\
&+\sum_{i=1}^{2}\sum_{j=1}^{2}g^2\psi_{ij}R_{kj}L^*_{\ell i}\frac{m_{\chi_i^+}m_{\chi_j^+}}{4\pi^2}f(m^2_{\chi_i^+},m^2_{\chi_j^+},m^2_{W^-})\\
&+0\\
&-\sum_{i=1}^{2}\sum_{j=1}^{2}\frac{m_\tau}{8\pi^2}G_{\tau ij}(\alpha_{\tau\ell}D_{\tau1i}-\gamma_{\tau\ell}D_{\tau2i})(\beta^*_{\tau k}D^*_{\tau1i}+\alpha_{\tau k}D^*_{\tau2j})f(m_\tau^2,m^2_{\tilde{\tau}_i},m^2_{\tilde{\tau}_j})
\end{aligned} \tag{38}$$

The corrections $\delta\tau_{k\ell}$ are given by

$$\delta\tau_{k\ell} = -\sum_{i=1}^{2}\sum_{j=1}^{2}\frac{m_t}{8\pi^2}E_{ji}(\beta_{t\ell}D_{t1j}+\alpha^*_{t\ell}D_{t2j})(\alpha^*_{tk}D^*_{t1i}-\gamma^*_{tk}D^*_{t2i})f(m_t^2,m^2_{\tilde{t}_i},m^2_{\tilde{t}_j})$$
$$-\sum_{i=1}^{2}\sum_{j=1}^{2}\frac{m_b}{8\pi^2}G_{ji}(\beta_{b\ell}D_{b1j}+\alpha^*_{b\ell}D_{b2j})(\alpha^*_{bk}D^*_{b1i}-\gamma^*_{bk}D^*_{b2i})f(m_b^2,m^2_{\tilde{b}_i},m^2_{\tilde{b}_j})$$
$$+0$$
$$+0$$
$$+\sum_{i=1}^{4}\sum_{j=1}^{4}\frac{g^3}{2\pi^2\cos^2\theta_W}S'_{ij}L'''_{kj}R'''_{i\ell}m_{\chi^0_i}m_{\chi^0_j}f(m^2_{\chi^0_i},m^2_{\chi^0_j},m_Z^2)$$
$$-\sum_{i=1}^{4}\sum_{j=1}^{4}\sum_{n=1}^{3}\frac{g^3}{4\pi^2}S'_{ij}\{Q'_{\ell i}(Y_{n1}+iY_{n3}\sin\beta)-S'_{\ell i}(Y_{n2}+iY_{n3}\cos\beta)\}$$
$$\{Q'_{jk}(Y_{n1}+iY_{n3}\sin\beta)-S'_{jk}(Y_{n2}+iY_{n3}\cos\beta)\}m_{\chi^0_i}m_{\chi^0_j}f(m^2_{\chi^0_i},m^2_{\chi^0_j},m^2_{H^0_n})$$
$$+\frac{g^3m_Z\cos\beta}{4\sqrt{2}\cos\theta_W}\sum_{i=1}^{4}\sum_{n=1}^{3}\sum_{m=1}^{3}\{Q'_{\ell i}(Y_{n1}+iY_{n3}\sin\beta)-S'_{\ell i}(Y_{n2}+iY_{n3}\cos\beta)\}$$
$$\{Q'_{ik}(Y_{m1}+iY_{m3}\sin\beta)-S'_{ik}(Y_{m2}+iY_{m3}\cos\beta)\}\{\tan\beta(Y_{n2}-iY_{n3}\cos\beta)(3Y_{m2}+iY_{m3}\cos\beta)$$
$$-4Y_{n1}(Y_{m2}-iY_{m3}\cos\beta)-2\tan\beta(Y_{m1}-iY_{m3}\sin\beta)(Y_{n1}+iY_{n3}\sin\beta)\}\frac{m_{\chi^0_i}}{16\pi^2}f(m^2_{\chi^0_i},m^2_{H^0_m},m^2_{H^0_n})$$
$$-\frac{2g^3m_Z\sin\beta}{\sqrt{2}\cos^3\theta_W}\sum_{i=1}^{4}L'''_{ki}R'''_{i\ell}\frac{m_{\chi^0_i}}{16\pi^2}f(m^2_{\chi^0_i},m_Z^2,m_Z^2)$$
$$-\sum_{i=1}^{2}\sum_{j=1}^{2}\epsilon'_{kj}\epsilon^*_{\ell i}\psi_{ij}\cos\beta\sin\beta\frac{m_{\chi^+_i}m_{\chi^+_j}}{16\pi^2}f(m^2_{\chi^+_i},m^2_{\chi^+_j},m^2_{H^-})$$
$$+\frac{gm_W}{2\sqrt{2}}\sum_{i=1}^{2}\epsilon'_{ki}\epsilon^*_{\ell i}\cos\beta\sin^2\beta(1+2\cos^2\beta+\cos2\beta\tan^2\theta_W)\frac{m_{\chi^+_i}}{16\pi^2}f(m^2_{\chi^+_i},m^2_{H^-},m^2_{H^-})$$
$$-\sum_{i=1}^{2}\frac{g^3}{\sqrt{2}}m_W\sin\beta R^*_{\ell i}L_{ki}\frac{m_{\chi^+_i}}{4\pi^2}f(m^2_{\chi^+_i},m^2_{W^-},m^2_{W^-})$$
$$+0$$
$$+0$$
$$-\sum_{i=1}^{2}\sum_{j=1}^{2}\frac{m_\tau}{8\pi^2}G_{\tau ij}(\beta_{\tau\ell}D_{\tau1i}+\alpha^*_{\tau\ell}D_{\tau2i})(\alpha^*_{\tau k}D^*_{\tau1j}-\gamma^*_{\tau k}D^*_{\tau2j})f(m_\tau^2,m^2_{\tilde{\tau}_i},m^2_{\tilde{\tau}_j}) \quad (39)$$

where G_{ij}, E_{ij}, h_t, ψ_{ij} and $G_{\tau ij}$ are given by

$$G_{ij} = \frac{gM_Z}{\sqrt{2}\cos\theta_W}((-\frac{1}{2}+\frac{1}{3}\sin^2\theta_W)D^*_{b1i}D_{b1j}-\frac{1}{3}\sin^2\theta_W D^*_{b2i}D_{b2j})\sin\beta$$
$$+\frac{gm_b\mu}{\sqrt{2}m_W\cos\beta}D^*_{b1i}D_{b2j}$$
$$E_{ij} = \frac{gM_Z}{\sqrt{2}\cos\theta_W}((\frac{1}{2}-\frac{2}{3}\sin^2\theta_W)D^*_{t1i}D_{t1j}+\frac{2}{3}\sin^2\theta_W D^*_{t2i}D_{t2j})\sin\beta$$

$$-\frac{gm_t^2}{\sqrt{2}m_W\sin\beta}(D^*_{t1i}D_{t1j}+D^*_{t2i}D_{t2j})-\frac{gm_tA_t}{\sqrt{2}m_W\sin\beta}D^*_{t2i}D_{t2j}$$

$$h_t=\frac{gm_t}{\sqrt{2}m_W\sin\beta},\psi_{jk}=-gU_{k1}V_{j2} \quad (40)$$

$$G_{\tau ij}=\frac{gM_Z}{\sqrt{2}\cos\theta_W}((-\frac{1}{2}+\sin^2\theta_W)D^*_{\tau 1i}D_{\tau 1j}-\sin^2\theta_W D^*_{\tau 2i}D_{\tau 2j})\sin\beta$$
$$+\frac{gm_\tau\mu}{\sqrt{2}m_W\cos\beta}D^*_{\tau 1i}D_{\tau 2j} \quad (41)$$

3 Neutral Higgs decays including loop effects

We summarize now the result of the analysis. Thus $\mathcal{L}_{eff}$ of Eq. (6) may be written as follows

$$\mathcal{L}_{eff}=H^0_m\overline{\chi^0_k}(\alpha^{mS}_{k\ell}+\gamma_5\alpha^{mP}_{k\ell})\chi^0_\ell+H.c \quad (42)$$

where

$$\alpha^{mS}_{k\ell}=\frac{1}{2\sqrt{2}}\{(Y_{m1}-iY_{m3}\sin\beta)(\theta_{k\ell}+\delta\theta_{k\ell}+\Delta\tau_{k\ell})+(Y_{m2}+iY_{m3}\cos\beta)(\tau_{k\ell}+\Delta\theta_{k\ell}+\delta\tau_{k\ell})\} \quad (43)$$

and where

$$\alpha^{mP}_{k\ell}=\frac{1}{2\sqrt{2}}\{(Y_{m2}+iY_{m3}\cos\beta)(\tau_{k\ell}+\delta\tau_{k\ell}-\Delta\theta_{k\ell})+(Y_{m1}-iY_{m3}\sin\beta)(-\theta_{k\ell}+\Delta\tau_{k\ell}-\delta\theta_{k\ell})\} \quad (44)$$

Next we discuss the implications of the above result for the decay of the neutral Higgs.

The partial width of the decay $H^0_m\to\chi^0_k\chi^0_\ell$ is given by

$$\Gamma_{mk\ell}(H^0_m\to\chi^0_k\chi^0_\ell)=\frac{1}{\pi M^3_{H^0_m}(1+\delta_{k\ell})}\sqrt{[(m^2_{\chi^0_\ell}+m^2_{\chi^0_k}-M^2_{H^0_m})^2-4m^2_{\chi^0_k}m^2_{\chi^0_\ell}]}$$
$$\{\frac{1}{2}(|\alpha^{mS}_{k\ell}|^2+|\alpha^{mP}_{k\ell}|^2)(M^2_{H^0_m}-m^2_{\chi^0_k}-m^2_{\chi^0_\ell})-\frac{1}{2}(|\alpha^{mS}_{k\ell}|^2-|\alpha^{mP}_{k\ell}|^2)(2m_{\chi^0_k}m_{\chi^0_\ell})\} \quad (45)$$

The neutral Higgs bosons can decay into different modes. However, there are important channels for this decay to occur, $\bar{b}b$, $\bar{t}t$, $\bar{s}s$, $\bar{c}c$, $\bar{\tau}\tau$, $\chi^+_i\chi^-_j$ and $\chi^0_i\chi^0_j$. The other channels of neutral Higgs decay are the decaying modes into the other fermions of the SM, squarks, sleptons, other Higgs bosons, W and Z boson pairs, one Higgs and a vector boson, $\gamma\gamma$ pairs and finally into the gluonic decay i.e, $H^0_m\to gg$. The lightest SM fermions channels could be ignored for the smallness of their couplings. We choose the region in the parameter space where we can ignore the other channels which either are not allowed kinematically or suppressed

by their couplings. Thus in this work, squarks and sleptons are too heavy to be relevant in neutral Higgs decay. The neutral Higgs decays into non-supersymmetric final states that involve gauge bosons and/or other Higgs bosons are ignored as well. In the region of large $\tan\beta$, these decays are very small and can be neglected as final states [21].

We calculate the radiative corrected partial decay widths of the important channels mentioned above. In the case of CP violating case under investigation we use the analysis of [2], for the radiatively corrected Γ of neutral Higgs into quarks, leptons and chargino pairs. For the radiatively corrected decay width into neutralino we use the current analysis. We define

$$\Delta\Gamma_{mk\ell} = \frac{\Gamma(H_m^0 \to \chi_k^0\chi_\ell^0) - \Gamma^0(H_m^0 \to \chi_k^0\chi_\ell^0)}{\Gamma^0(H_m^0 \to \chi_k^0\chi_\ell^0)} \tag{46}$$

where the first term in the numerator is the decay width including the full loop corrections and the second term is the decay width evaluated at the tree level. Finally to investigate the size of the loop effects on the branching ratios of the neutral Higgs decay we define the following quantity

$$\Delta Br_{mk\ell} = \frac{Br(H_m^0 \to \chi_k^0\chi_\ell^0) - Br^0(H_m^0 \to \chi_k^0\chi_\ell^0)}{Br^0(H_m^0 \to \chi_k^0\chi_\ell^0)} \tag{47}$$

where the first term in the numerator is the branching ratio including the full loop corrections and the second term is the branching ratio evaluated at the tree level. The analysis of this section is utilized in Sec.(4) where we give a numerical analysis of the size of the loop effects and discuss the effect of the loop corrections on the branching ratios.

4 NUMERICAL ANALYSIS

In this section we investigate the size of the loop corrections on the partial decay widths and the branching ratios of the neutral Higgs bosons decay into neutralinos. The analysis of Sec. 2 and Sec. 3 is quite general and valid for the minimal supersymmetric standard model. For the sake of numerical analysis we will limit the parameter space by working within the framework of the SUGRA model [22]. Specifically we will work within the framework of the the extended nonuniversal mSUGRA model including CP phases. We take as our parameter space at the grand unification scale to be the following: the universal scalar mass m_0, the universal gaugino mass $m_{1/2}$, the universal trilinear coupling $|A_0|$, the ratio of

the Higgs vacuum expectation values $\tan\beta =< H_2 > / < H_1 >$ where H_2 gives mass to the up quarks and H_1 gives mass to the down quarks and the leptons. In addition, we take for CP phases the following: the phase θ_μ of the Higgs mixing parameter μ, the phase α_{A_0} of the trilinear coupling A_0 and the phases $\xi_i (i = 1, 2, 3)$ of the $SU(3)_C$, $SU(2)_L$ and $U(1)_Y$ gaugino masses. In this analysis the electroweak symmetry is broken by radiative effects which allows one to determine the magnitude of μ by fixing M_Z. In the analysis we use one loop renormalization group (RGEs) equations for the evolution of the soft SUSY breaking parameters and for the parameter μ, and two loop RGEs for the gauge and Yukawa couplings. In the numerical analysis we compute the loop corrections and also analyze their dependence on the phases. The masses of particles involved in the analysis are ordered as follows: for neutralinos $m_{\chi_1^0} < m_{\chi_2^0} < m_{\chi_3^0} < m_{\chi_4^0}$ and for the neutral Higgs $(m_{H_1}, m_{H_2}, m_{H_3}) \to (m_H, m_h, m_A)$ in the limit of no CP mixing where m_H is the heavy CP even Higgs, m_h is the light CP even Higgs, and m_A is the CP odd Higgs.

We first discuss the size of the loop corrections of the partial decay width defined in Eq.(46). As was mentioned before, the loop corrected partial widths of the neutral Higgs decay into neutralinos have been investigated in the absence of CP violating phases [16, 17]. The magnitude of the corrections in these analyses is of the order of $\sim 10\%$ of the tree level value. The current analysis supports this result. In Fig. (3) , we give a plot of $\Delta\Gamma_{113}$ as functions of $\tan\beta$ for the specific set of inputs given in the figure caption. We notice that the partial decay width gets a change of $2 \sim 12\%$ of its tree level value. The role played by $\tan\beta$ in this analysis is complicated and is coming from different regions in the analysis. First of all, it affects the spectrum and couplings of neutral Higgs with neutralinos at tree level through the diagonalizing matrices of both neutral Higgs bosons and neutralino. We also find that $\tan\beta$ is playing a crucial rule at the one loop level analysis. The neutral Higgs mass^2 matrix receives corrections from the stop, sbottom, chargino and neutralino sectors and these corrections are sensitive to the value of $\tan\beta$. We also see the explicit and implicit effects of $\tan\beta$ in the loop corrected couplings of neutralinos with neutral Higgs presented in Eq. (43) and Eq. (44) for $\alpha_{k\ell}^{mS}$ and $\alpha_{k\ell}^{mP}$ respectively. We also notice that the CP violating phase θ_μ can affect the value of this change. This effect has not been discussed in the previous analyses because these analyses have been carried out for the CP conservation case. We can also trace down the role played by the phase θ_μ in the analysis. We can see

that, θ_μ affects the tree level of analysis through its presence in the neutralino mass matrix and at loop level where it can produce mixing in the neutral Higgs sector and also affects the radiative corrected couplings between the neutralinos and neutral Higgs bosons. In the limit where CP violating phases are set to zero and by using the same inputs of [16], we were able to have a fair agreement with with their Figs. 2-4, 6. In the work of [17] only 8 out of 28 diagrams of the current analysis are calculated. By including these diagrams only in the comparison, our analysis is in fair agreement with their Figs.2, 3, 5, 7 and 9 for their inputs.

Now we compute the loop correction effects of the branching ratios of the neutral Higgs decays into neutralinos. The branching ratio of a decay mode is the ratio between the partial decay rate of this mode and the total decay rate for all possible channels. In the parameter space we are investigating, these channels are decays into charginos, heavy quarks, taus, and neutralinos. In Figs. (4) and (5) we give a plot of $\Delta Br_1 \to \chi_2^0\chi_2^0$ and $\Delta Br_3 \to \chi_1^0\chi_3^0$ as functions of $m_{1/2}$ for the specific set of inputs given in the captions of these figures. We first notice that the loop correction of the branching ratios can reach as high as 35% of the tree level value for the case of H_1 boson and as high as 55% for the case of H_3 boson. We also can see the effect of the CP violating phase θ_μ in these two figures. In the branching ratio study, this CP violating phase can affect many decay modes of neutral Higgs into different quarks and leptons via radiative corrections of these modes. It can affect both tree and loop level of the analysis in the cases of decays into charginos and neutralinos due to the presence of the parameter μ in the chargino, neutralino and sfermion mass matrices. The role played by the parameter $m_{1/2}$ is mainly through the chargino and neutralino mass matrices since the gaugino masses $\tilde{m}_1$ and $\tilde{m}_2$ are originating from $m_{1/2}$ at GUT scale. The parameter $m_{1/2}$ is also affecting the evolution of the other soft supersymmetry breaking parameters like the trilinear couplings A_f from GUT scale down to the electroweak scale.

In Figs. (6) and (7) we give a plot of $\Delta Br_1 \to \chi_1^0\chi_2^0$ and $\Delta Br_3 \to \chi_2^0\chi_2^0$ as functions of θ_μ for the specific set of inputs given in the captions of these figures. We notice in these two figures that the loop corrections of the branching ratios for these modes can reach as high as 35% of the tree level value. We see here again the effect of the CP violating phase θ_μ on the corrections of branching ratio for these decay modes. In the case of H_3 decay, one can see that θ_μ affects not only the magnitude of $\Delta Br_3 \to \chi_2^0\chi_2^0$ but also its sign depending on θ_μ. The analysis of these two figures also shows the importance of the parameter $\tan\beta$ in the loop

corrections for these the branching ratios. This parameter is important at tree level through neutral Higgs couplings with different quarks and leptons and through the diagonalization of the neutral Higgs, chargino and neutralino mass matrices. At one loop level, it affects both neutral Higgs spectrum and couplings with different fields.

In Figs. (8) and (9) we give a plot of $\Delta Br_1 \to \chi_1^0\chi_3^0$ and $\Delta Br_3 \to \chi_1^0\chi_2^0$ as functions of α_0 for the specific set of inputs given in the captions of these figures. We notice in these two figures that the loop correction of the branching ratios for these modes can reach as high as 40% of the tree level. The effects of the magnitude of $|A_0|$ and its CP violating phase are clear in both modes and could be understood form the effect of the trilinear couplings on the squark and slepton mass^2 matrices in the stop case through A_t, in the sbottom case through A_b, in the stau case through the parameter A_τ.

In Figs. (10) and (11) we give a plot of $\Delta Br_1 \to \chi_1^0\chi_3^0$ and $\Delta Br_3 \to \chi_1^0\chi_2^0$ as functions of ξ_2 for the specific set of inputs given in the captions of these figures. Here we find that ξ_2 phase has a smaller effect on the loop corrections. The reason for this could be understood qualitatively from the fact that the chargino and neutralino loops that carry the effect of this phase are correcting the tree level of the analysis less than that of the other loops in this region of the parameter space.

5 RELEVANCE OF RESULTS AT LHC

The production of the MSSM Higgs particles at the Large Hadron Collider LHC ($\sqrt{s}$ = 14 TeV) occurs via gluon fusion $gg \to H_i$ and the associated production mechanism $gg + q\bar{q} \to b\bar{b}H_i$. The cross section of these processes can reach few tens of pb at large $\tan\beta$ region and for a moderate Higgs masses $\sim$ 500 GeV. For integrated luminosity (10) 100 fb^{-1} in the (low) high luminosity option, σ = 1 pb would correspond to (10^4) 10^5 events [23]. These Higgs particles once produced, can decay into many channels and one of them is the channel considered here, the neutralino one.

The decay of the heavy MSSM Higgs bosons to neutralinos could be observed at LHC. When χ^0 decay channels are open, their branching ratios can be close to $\sim$ 20% [24] and that gives an opportunity for experimental analysis of the MSSM parameter space. The authors of [25], study the decays of H_1 and H_3 after their production at LHC into two next-to-lightest neutralinos χ_2^0, with each of the neutralinos in turn decaying to two Standard Model fermions along with

the lightest neutralino χ_1^0, assumed to be the lightest supersymmetric particle (the LSP) and carries missing energy. The two fermions will most often be quarks, leading to two jets and missing E_T in the final state. To obtain a clean signature, one should only focus on the case where the two SM fermions are leptons. Thus the process under consideration is

$$H_1, H_3 \to \chi_2^0 \chi_2^0 \to 4\ell^\pm + E_T^{miss} \quad (\ell = e, \mu) \tag{48}$$

The above process provides a clear signature containing two pairs of leptons with opposite sign and same flavor, in addition to a substantial amount of missing energy due to the escaping lightest neutralino. In their analysis, the authors of [25] show that one can distinguish this signal from the (mainly SUSY) background for values of $\tan\beta = 5 - 40$. Their analysis for the decay of Heavy Higgs bosons into neutralinos is based on the HDECAY package [26]. This analysis does not take into account the loop corrections of the neutral Higgs vertices with neutralinos and is carried out in the CP conserving scenario. They also study the decay of neutralinos into leptons in the limit of vanishing CP phases. In the case (2) of the first paper of [25], the author used the inputs $M_2 = 180$, $M_1 = 100$, $\mu = 500$, $m_{\tilde{\ell}} = 250$ and $M_{\tilde{q},\tilde{g}} = 1000$ GeV. It is shown in Fig. (6) of [25], for integrated luminosity of 100 fb^{-1}, that the expectation to discover the Higgs bosons with a clear and visible signature over the background occurs for $m_A = 380$ GeV and $\tan\beta = 10$. Now by putting these parameters by hand in our analysis with setting all the CP phases to zero, we get for ΔBr_{322}, defined by Eq. (47), the value of $\sim -25\%$. So the tree value of the branching ratio that was used in the analysis of [25] would have been suppressed by radiative corrections of the above percentage and that would of course change the output of the analysis.

In the analysis of [27], the authors investigate the same four-lepton signal with missing energy at LHC. In their top Fig. 3, they use for their inputs, $\tan\beta = 20$, $M_1 = \frac{5}{3}\tan^2\theta_W M_2$, $m_A = 400$, $m_{\tilde{\ell}} = 150$, $M_{\tilde{q}} = 1000$, $M_{\tilde{g}} = 800$, $A_\tau = A_l = 0$ and $m_{\tilde{\tau}} = 250$ GeV. For the parameter point $\mu = -200$ GeV and $M_2 = 200$ GeV, one has $\sigma(pp \to H_1, H_3) \times Br(H_1, H_3 \to 4\ell + E_T^{miss}) = 37fb$. Thus for an integrated luminosity of $100fb^{-1}$, the event number can reach 3700 events before applying selection cuts. In this figure and for this point, the four-lepton signal originates mainly through $\chi_2^0\chi_2^0$ channel. By calculating the corrections to the branching ratios in our analysis for this input but with no CP violating phases, one finds that the branching ratio corrections ΔBr_{322} and ΔBr_{122} are $+28\%$ and $+24\%$ respectively. The authors of [27] did not take into account the loop corrections to

the branching ratios of neutral Higgs into the neutralino and thus the inclusion of these corrections in their analysis would enhance the event number at LHC.

We note further, that the couplings of the Higgs bosons to the SM particles and their supersymmetric partners are modified by the CP violation phases. The Higgs boson masses and their CP properties are modified as well from those predicted in the CP conserving case. Thus the cross sections for MSSM Higgs particles production and their decay signatures could also be much more complicated than in the CP preserving scenario. So an analysis that considers the Higgs bosons production and their detection in the environment of LHC with CP violating phases would be much more involved and is beyond the scope of this paper.

6 CONCLUSION

In this paper we have worked out the loop corrections to $\chi^0_k\chi^0_\ell H^0_m$ couplings within MSSM. This analysis extends previous analysis of supersymmetric loop corrections to the couplings of neutral Higgs bosons with charginos and with standard model fermions within minimal supersymmetric standard models including the full set of allowed CP phases. The result of the analysis is then applied to the computation of the decay of the neutral Higgs bosons to neutralino pairs. In the absence of loop corrections, the lightest Higgs boson mass is less than M_Z and including these corrections can lift the lightest Higgs mass above M_Z. In the CP invariance scenario the spectrum of the neutral Higgs sector consists of two CP even Higgs bosons and one CP odd Higgs boson. With the inclusion of CP phases, the Higgs boson mass eigenstates are no longer CP even and CP odd states when loop corrections to the Higgs boson mass matrix are included. Further, inclusion of loop corrections to the couplings of neutralinos with neutral Higgs is in general dependent on CP phases. Thus the decays of neutral Higgs into neutralinos can be sensitive to the loop corrections and to the CP violating phases. The effect of the supersymmetric loop corrections is found to to be in the range of $\sim 10\%$ for the partial decay width. For the branching ratios it is found to be be rather large, as much as 50% in some regions of the parameter space. The effect of CP phases on the modifications of the partial decay width and the branching ratio is found to be substantial in some regions of the MSSM parameter space. Specific attention is paid to the neutralino decay mode that can lead to a four-lepton signal.

References

[1] M. Carena and H. E. Haber, Prog. Part. Nucl. Phys. **50**, 63 (2003).

[2] T. Ibrahim and P. Nath, Phys. Rev. D **68**, 015008 (2003); T. Ibrahim, Phys. Rev. D **76**, 075012 (2007) [arXiv:0704.1913 [hep-ph]].

[3] P. Nath, Phys. Rev. Lett.**66**, 2565 (1991); Y. Kizukuri and N. Oshimo, Phys.Rev. **D 46**,3025 (1992). T. Ibrahim and P. Nath, Phys. Lett. B **418**, 98 (1998); Phys. Rev. **D 57**, 478(1998); Phys. Rev. **D 58**, 111301 (1998); T. Falk and K Olive, Phys. Lett. **B 439**, 71 (1998); M. Brhlik, G.J. Good, and G.L. Kane, Phys. Rev. **D 59**, 115004 (1999); A. Bartl, T. Gajdosik, W. Porod, P. Stockinger, and H. Stremnitzer, Phys. Rev. **D 60**, 073003 (1999); S. Pokorski, J. Rosiek and C.A. Savoy, Nucl.Phys. **B 570**, 81 (2000); E. Accomando, R. Arnowitt and B. Dutta, Phys. Rev. **D 61**, 115003 (2000); U. Chattopadhyay, T. Ibrahim, D.P. Roy, Phys.Rev. **D 64**, 013004 (2001).

[4] C. S. Huang and W. Liao, Phys. Rev. **D 61**, 116002 (2000); Phys. Rev. **D 62**, 016008 (2000); A. Bartl, T. Gajdosik, E. Lunghi, A. Masiero, W. Porod, H. Stremnitzer and O. Vives, hep-ph/0103324; M. Brhlik, L. Everett, G. Kane and J. Lykken, Phys. Rev. Lett. **83**, 2124, 1999; Phys. Rev. **D 62**, 035005 (2000); E. Accomando, R. Arnowitt and B. Dutta, Phys. Rev. **D 61**, 075010 (2000); T. Ibrahim and P. Nath, Phys. Rev. **D 61**, 093004 (2000).

[5] T. Falk, K.A. Olive, M. Prospelov, and R. Roiban, Nucl. Phys. **B 560**, 3 (1999); V. D. Barger, T. Falk, T. Han, J. Jiang, T. Li and T. Plehn, Phys. Rev. **D 64**, 056007 (2001); S.Abel, S. Khalil, O.Lebedev, Phys. Rev. Lett. **86**, 5850 (2001); T. Ibrahim and P. Nath, Phys. Rev. **D 67**, 016005 (2003) arXiv:hep-ph/0208142; D. Chang, W-Y.Keung,and A. Pilaftsis, Phys. Rev. Lett. **82**, 900 (1999).

[6] E. Commins et al., Phys. Rev. **A 50**, 2960 (1994)

[7] P. G. Harris et al., Phys. Rev. Lett. **82**, 904 (1999)

[8] S. K. Lamoreaux, J. P. Jacobs, B. R. Heckel, F. J. Raab, and E. N. Forston, Phys. Rev. Lett. **57**, 3125 (1986).

[9] T. Ibrahim and P. Nath, arXiv:0705.2008 [hep-ph].

[10] A. Pilaftsis, Phys. Rev. **D58**, 096010 (1998); Phys. Lett.**B 435**, 88 (1998); A. Pilaftsis and C.E.M. Wagner, Nucl. Phys. **B 553**, 3 (1999); D.A. Demir, Phys. Rev. **D 60**, 055006 (1999); S. Y. Choi, M. Drees and J. S. Lee, Phys. Lett. **B 481**, 57 (2000); T. Ibrahim, Phys. Rev. **D 64**, 035009 (2001). S. W. Ham, S. K. Oh, E. J. Yoo, C. M. Kim and D. Son, arXiv:hep-ph/0205244; M. Boz, Mod. Phys. Lett. **A 17**, 215 (2002). M. Carena, J. R. Ellis, A. Pilaftsis and C. E. Wagner, Nucl. Phys. **B 625**, 345 (2002), [arXiv:hep-ph/0111245]. J. Ellis, J. S. Lee and A. Pilaftsis, arXiv:hep-ph/0404167, E. Chrisova, H. Eberl, W. Majerotto, and S. Kraml, J. High Energy Phys. 12 (2002)021; E. Christova, H. Eberl, W. Majerotto, and S. Kraml, Nucl. Phys. **B 639**, 263(2002); **647**, 359(E) (2002) T. Ibrahim, P. Nath, Phys and A. Psinas. Rev. D **70**, 035006(2004). D. A. Demir, Phys. Rev. **D 60**, 055006 (1999); T. Ibrahim and P. Nath, Phys. Rev. **D 63**, 035009 (2001); Phys. Rev. **D 66**, 015005 (2002).

[11] K. S. Babu and C. F. Kolda, Phys. Lett. **B 451**, 77, 1999.

[12] T. Ibrahim, P. Nath, Phys. Rev. **D 68**, 015008(2003).

[13] D. A. Demir and K. A. Olive, Phs. Rev. **D 65**, 034007 (2002); G. Degrassi, P. Gambino, and G. F. Giudice, J. High Energy Phys. **12**, 009(2000); G. Belanger, F. Boudjema, A. Pukhov, and A. Semenov, Comput. Phys. Commun. **149**, 103(2002).

[14] T. Ibrahim, P. Nath, Phys. Rev. **D 69**, 075001(2004)

[15] T. Ibrahim, P. Nath and A. Psinas, Phys. Rev. **D 70**, 035006(2004).

[16] H. Eberl, M. Kncel, W. Majerotto, Y. Yamada, Nucl. Phys. **B 625** (2002) 372; H. Eberl, hep-ph/0410209.

[17] Z. Ren-You, M. Wen-Gan, W. Lang-Hui and J. Yi, Phys. Rev. **D 65**, 075018(2002).

[18] D. A. Demir, Phys. Rev. **D 60**, 055006(1999).

[19] T. Ibrahim, P. Nath, Phys. Rev. **D 63**, 035009(2001).

[20] T. Ibrahim, P. Nath, Phys. Rev. **D 66**, 015005(2002).

[21] J. F. Gunion, H. E. Haber, Nucl. Phys. B **307**, 445 (1988); A. Djouadi, hep/ph/9712334.

[22] A. H. Chamseddine, R. Arnowitt, and P. Nath, Phys. Rev. Lett. **49**, 970(1982); R. Barbieri, S. Ferrara, and C. A. Savoy, Phys. Lett. **B 119**, 343(1982); L. Hall, J. Lykken, and S. Weinberg, Phys. Rev. **D 27**, 2359(1983); P. Nath, R. Arnowitt, and A. H. Chamseddine, Nucl. Phys. **B 227**, 121(1983).

[23] A. Djouadi, hep-ph/0205248, Pramana 60 (2003) 215-238.

[24] A. Djouadi, P. Janot, J. Kalinowski and P.M. Zerwas, Phys.Lett. **B 376** (1996) 220-226

[25] F. Moortgat, hep-ph/0105081, proceedings for the 36th Rencontres de Moriond, QCD and High Energy Hadronic Interactions, Les Arcs, France, March 17 - 24, 2001; F. Moorgat, S. Abdullin and D. Denegri, hep-ph/0112046; LHC/LC Study Group, hep-ph/0410364, Phys. Rep. 426, 47(2006).

[26] A. Djouadi, J. Kalinowski, and M. Spira, Comp. Phys. Commun. **108**, 56 (1998).

[27] M. Bisset, J. Li, N. Kersting, F. Moortgat and S. Moritti, hep-ph/0709.1029.

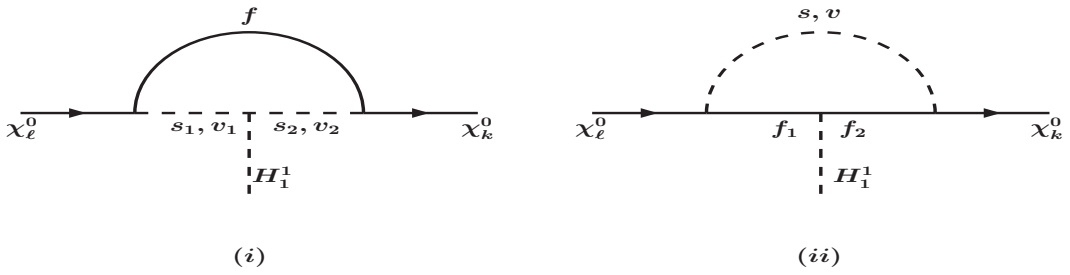

Figure 1: Set of diagrams contributing to radiative corrections $\delta\theta_{k\ell}$ and $\Delta\tau_{k\ell}$. (i): (a) $s_1 = \tilde{t}^*_j$, $s_2 = \tilde{t}^*_i$, $f = t$; (b) $s_1 = \tilde{b}^*_j$, $s_2 = \tilde{b}^*_i$, $f = b$; (c) $s_1 = H^0_n$, $s_2 = H^0_m$, $f = \chi^0_i$; (d) $v_1 = Z^0$, $v_2 = Z^0$, $f = \chi^0_i$; (e) $s_1 = H^-$, $s_2 = H^-$, $f = \chi^+_i$; (f) $v_1 = W^-$, $v_2 = W^-$, $f = \chi^+_i$; (g)$s_1 = \tilde{\tau}^*_i$, $s_2 = \tilde{\tau}^*_j$, $f = \tau$. (ii): (a) $f_1 = t$, $f_2 = t$, $s = \tilde{t}^*_j$; (b) $f_1 = b$, $f_2 = b$, $s = \tilde{b}^*_j$; (c)$f_1 = \chi^0_i$, $f_2 = \chi^0_j$, $v = Z^0$; (d) $f_1 = \chi^0_i$, $f_2 = \chi^0_j$, $s = H^0_n$; (e) $f_1 = \chi^+_i$, $f_2 = \chi^+_j$, $s = H^-$; (f) $f_1 = \chi^+_i$, $f_2 = \chi^+_j$, $v = W^-$; (g) $f_1 = \tau$, $f_2 = \tau$, $s = \tilde{\tau}^*_i$.

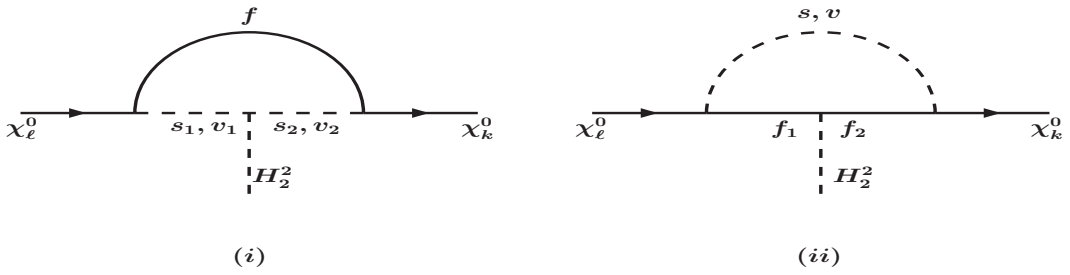

Figure 2: Set of diagrams contributing to radiative corrections $\Delta\theta_{k\ell}$ and $\delta\tau_{k\ell}$. (i): (a) $s_1 = \tilde{t}^*_j$, $s_2 = \tilde{t}^*_i$, $f = t$; (b) $s_1 = \tilde{b}^*_j$, $s_2 = \tilde{b}^*_i$, $f = b$; (c) $s_1 = H^0_n$, $s_2 = H^0_m$, $f = \chi^0_i$; (d) $v_1 = Z^0$, $v_2 = Z^0$, $f = \chi^0_i$; (e) $s_1 = H^-$, $s_2 = H^-$, $f = \chi^+_i$; (f) $v_1 = W^-$, $v_2 = W^-$, $f = \chi^+_i$; (g)$s_1 = \tilde{\tau}^*_i$, $s_2 = \tilde{\tau}^*_j$, $f = \tau$. (ii): (a) $f_1 = t$, $f_2 = t$, $s = \tilde{t}^*_j$; (b) $f_1 = b$, $f_2 = b$, $s = \tilde{b}^*_j$; (c)$f_1 = \chi^0_i$, $f_2 = \chi^0_j$, $v = Z^0$; (d) $f_1 = \chi^0_i$, $f_2 = \chi^0_j$, $s = H^0_n$; (e) $f_1 = \chi^+_i$, $f_2 = \chi^+_j$, $s = H^-$; (f) $f_1 = \chi^+_i$, $f_2 = \chi^+_j$, $v = W^-$; (g) $f_1 = \tau$, $f_2 = \tau$, $s = \tilde{\tau}^*_i$.

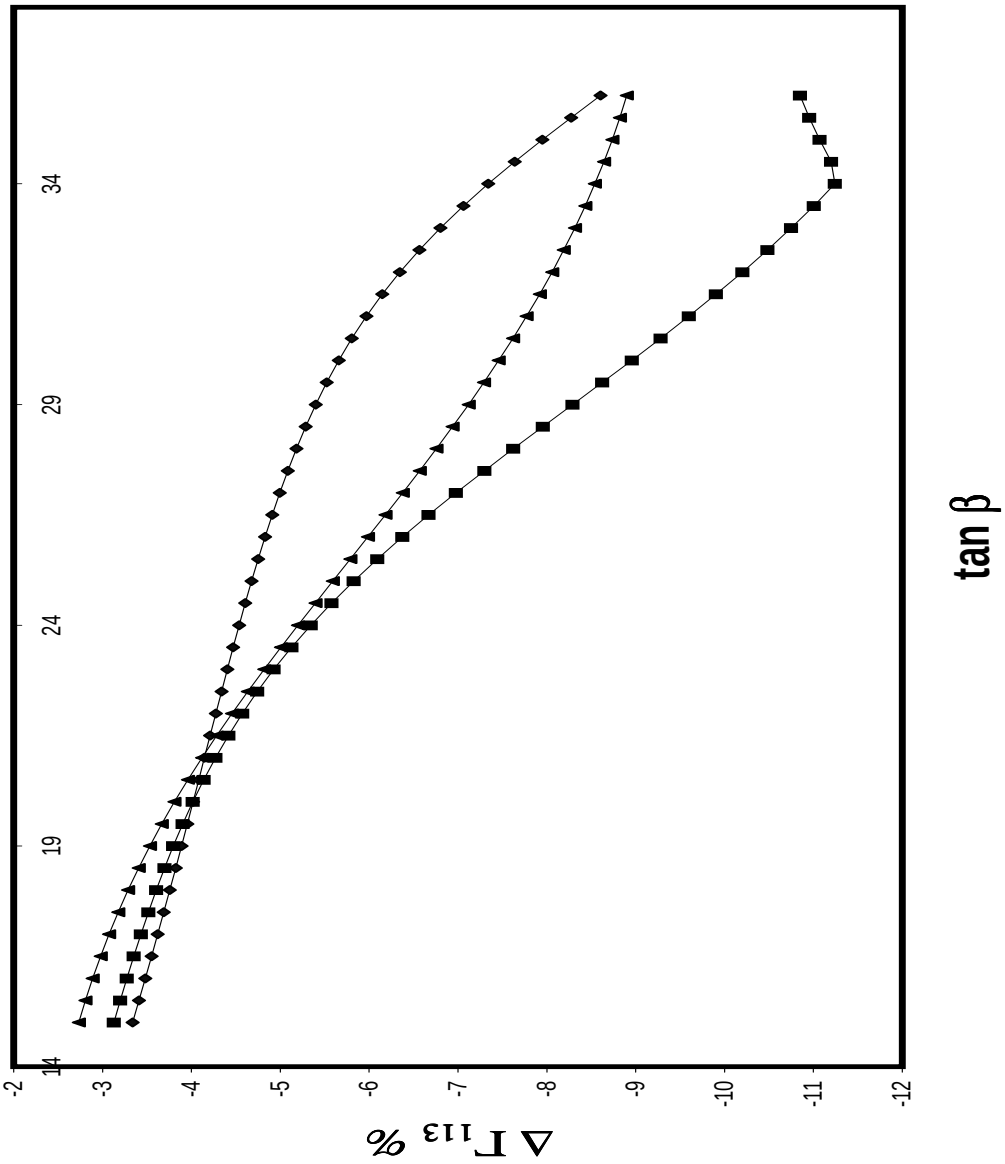

Figure 3: $\tan\beta$ dependence of $\Delta\Gamma_1 \to \chi_1^0\chi_3^0$. The curves in ascending order of the absolute value at $\tan\beta = 15$ correspond to $\theta_\mu = 0.7$, 0.2 and 0.0 rad. The input is $m_0 = 300$ GeV, $m_{1/2} = 100$ GeV, $|A_0| = 100$ GeV, $\xi_1 = 0.5$ (rad), $\xi_2 = 0.6$ (rad), $\xi_3 = 0.7$ (rad) and $\alpha_0 = 2.0$ (rad).

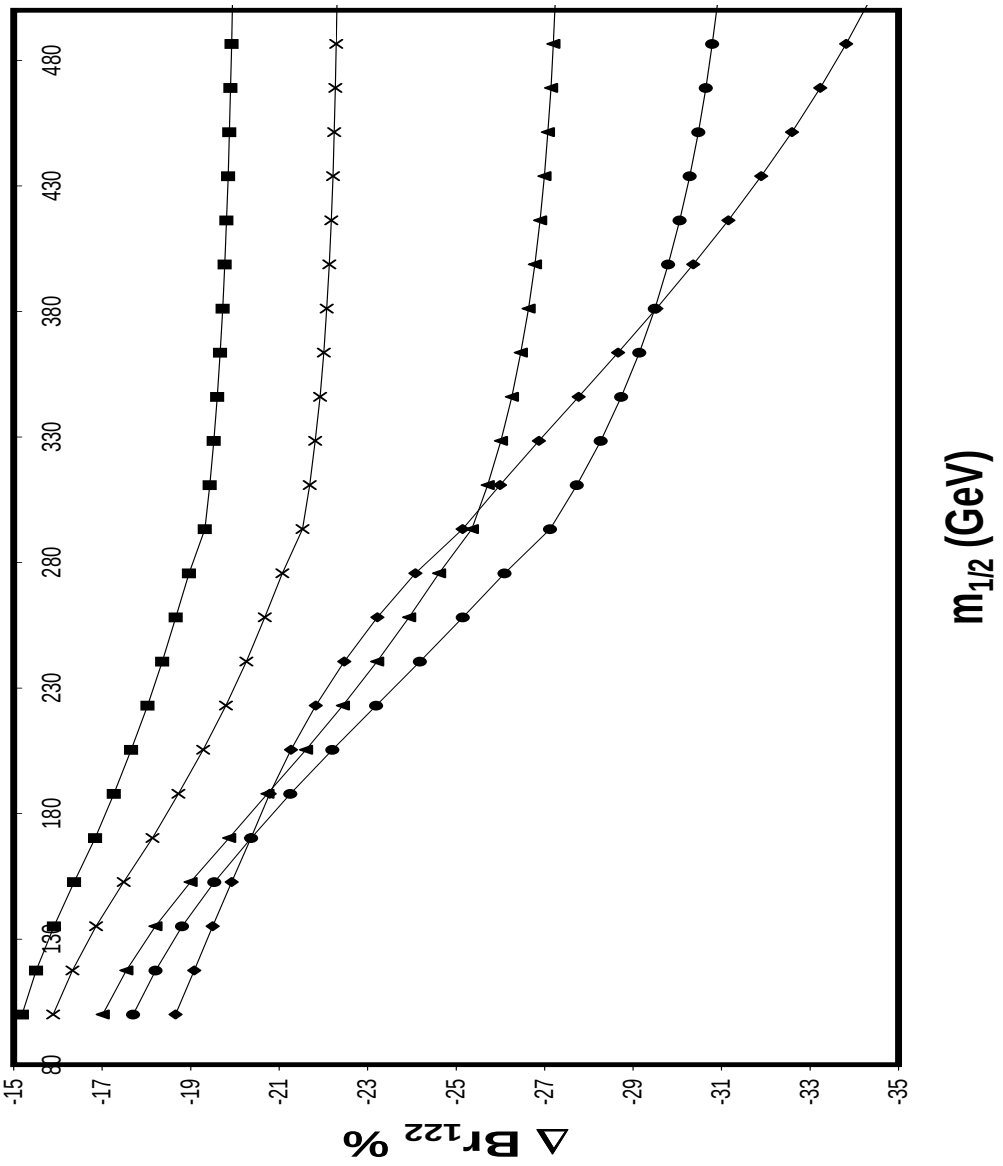

Figure 4: $m_{1/2}$ dependence of $\Delta Br_1 \to \chi_2^0\chi_2^0$. The curves in ascending order of the absolute value at $m_{1/2} = 100$ (GeV) correspond to $\theta_\mu = 1.2$, 1.0, 0.7, 0.5 and 0.2 rad. The input is $\tan\beta = 20$, $m_0 = 500$ GeV, $|A_0| = 250$ GeV, $\xi_1 = 0.4$ (rad), $\xi_2 = 0.5$ (rad), $\xi_3 = 0.6$ (rad) and $\alpha_0 = 0.8$ (rad).

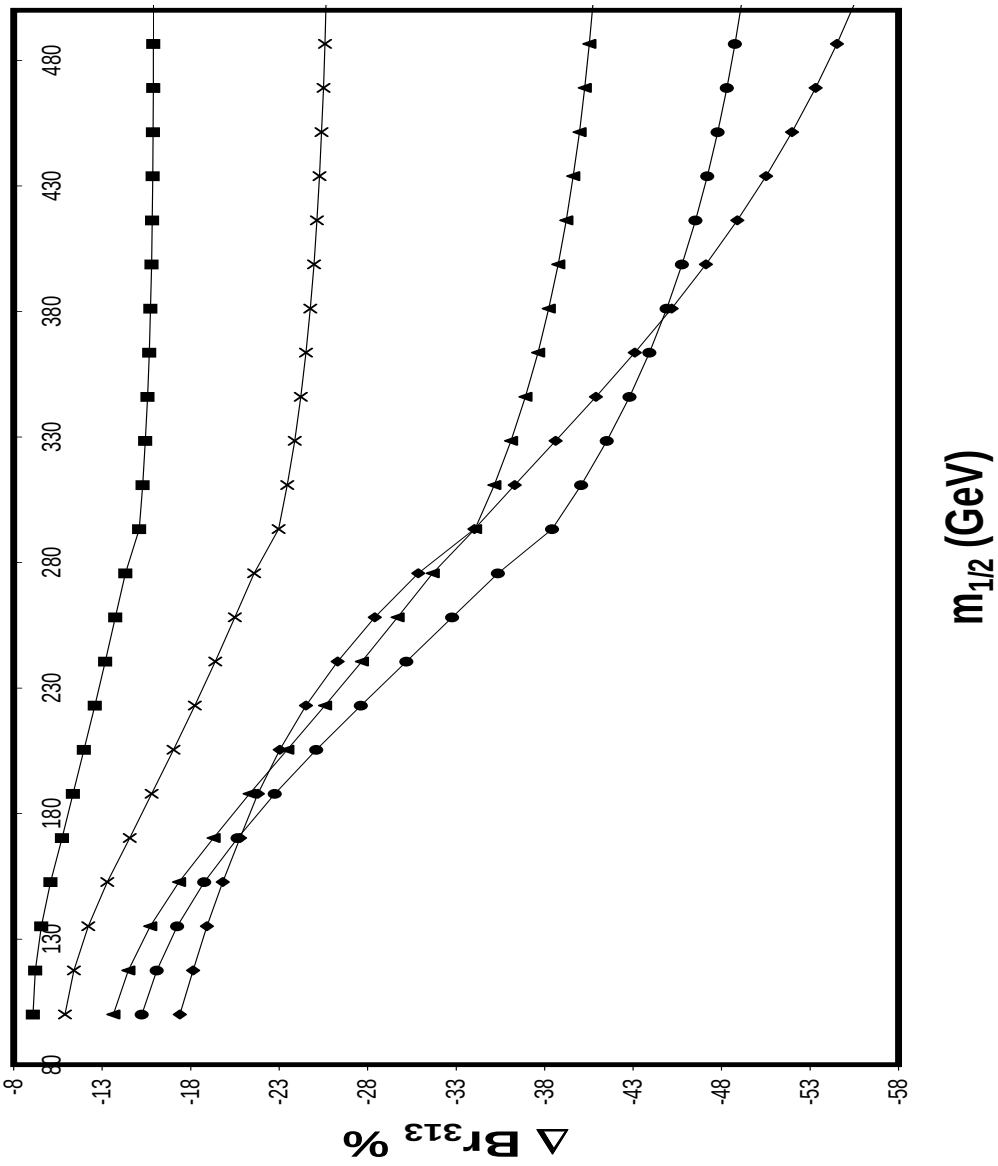

Figure 5: $m_{1/2}$ dependence of $\Delta Br_3 \to \chi_1^0\chi_3^0$. The curves in ascending order of the absolute value at $m_{1/2} = 100$ (GeV) correspond to $\theta_\mu = 1.2$, 1.0, 0.7, 0.5 and 0.2 rad. The input is $\tan\beta = 20$, $m_0 = 500$ GeV, $|A_0| = 250$ GeV, $\xi_1 = 0.4$ (rad), $\xi_2 = 0.5$ (rad), $\xi_3 = 0.6$ (rad) and $\alpha_0 = 0.8$ (rad).

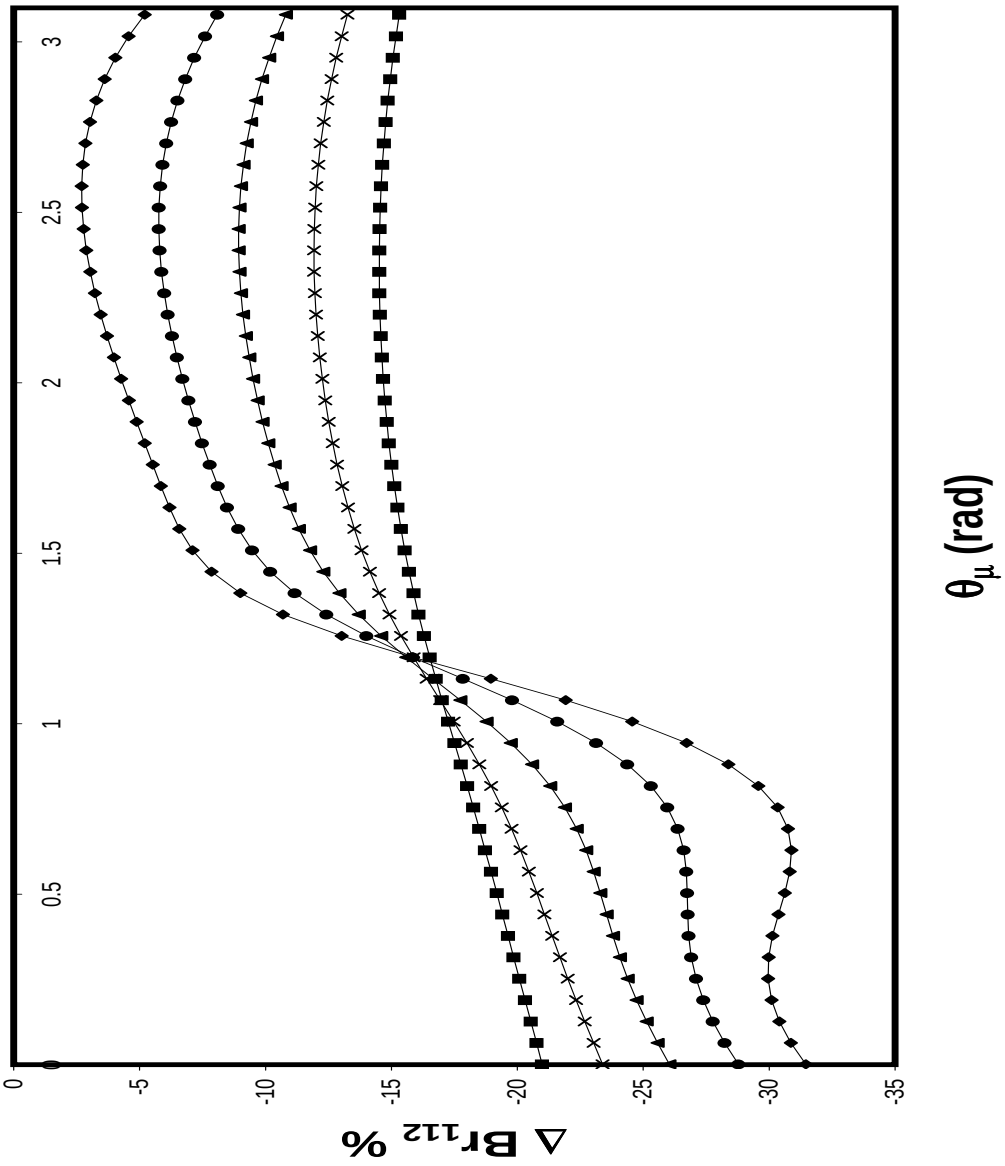

Figure 6: θ_μ dependence of $\Delta Br_1 \to \chi_1^0\chi_2^0$. The curves in descending order of the absolute value at $\theta_\mu = 0.0$ (rad) correspond to $\tan\beta = 40$, 35, 30, 25 and 20. The input is $m_{1/2} = 150$ GeV, $m_0 = 600$ GeV, $|A_0| = 600$ GeV, $\xi_1 = 0.3$ (rad), $\xi_2 = 0.4$ (rad), $\xi_3 = 0.5$ (rad) and $\alpha_0 = 0.5$ (rad).

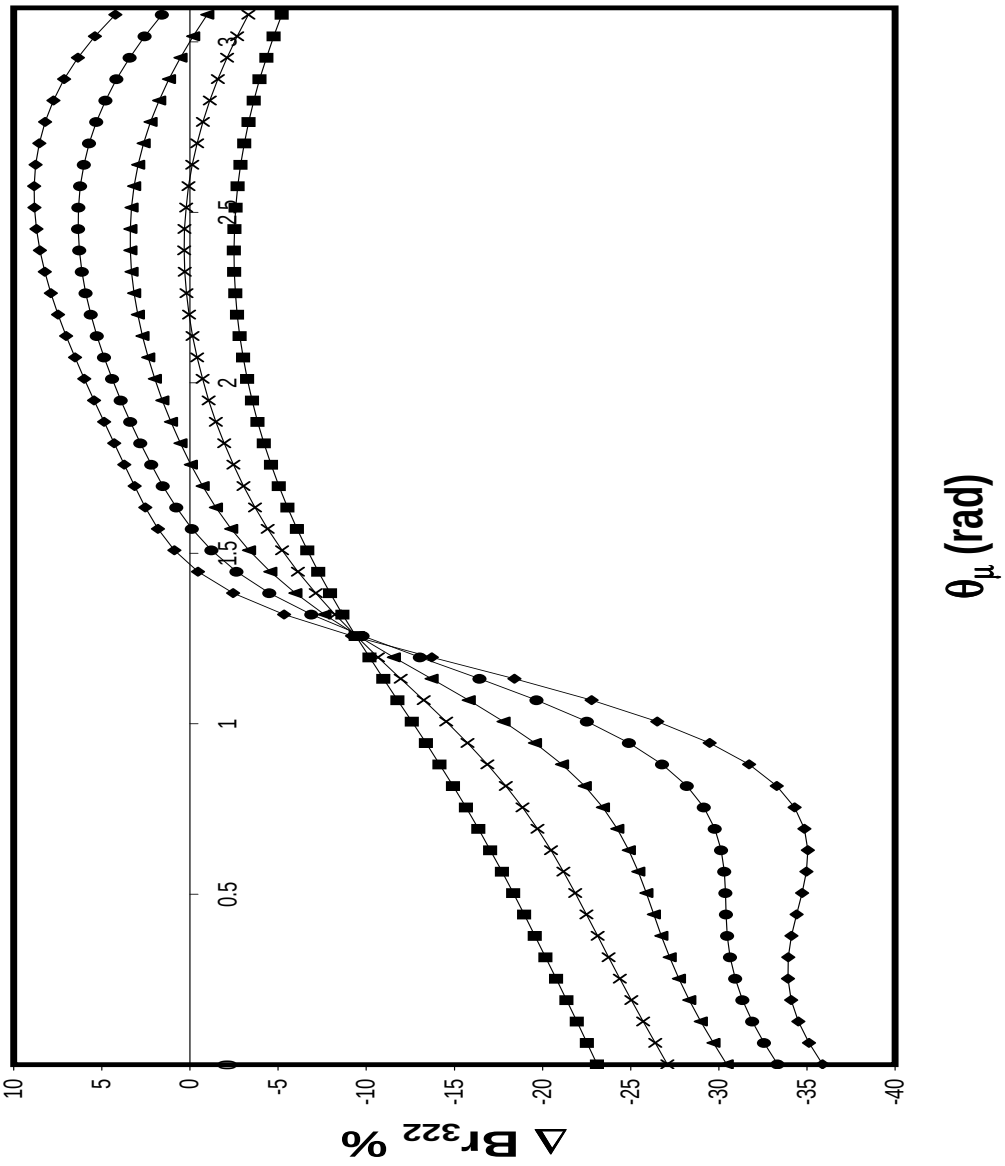

Figure 7: θ_μ dependence of $\Delta Br_3 \to \chi_2^0\chi_2^0$. The curves in descending order of the absolute value at $\theta_\mu = 0.0$ (rad) correspond to $\tan\beta = 40$, 35, 30, 25 and 20. The input is $m_{1/2} = 150$ GeV, $m_0 = 600$ GeV, $|A_0| = 600$ GeV, $\xi_1 = 0.3$ (rad), $\xi_2 = 0.4$ (rad), $\xi_3 = 0.5$ (rad) and $\alpha_0 = 0.5$ (rad).

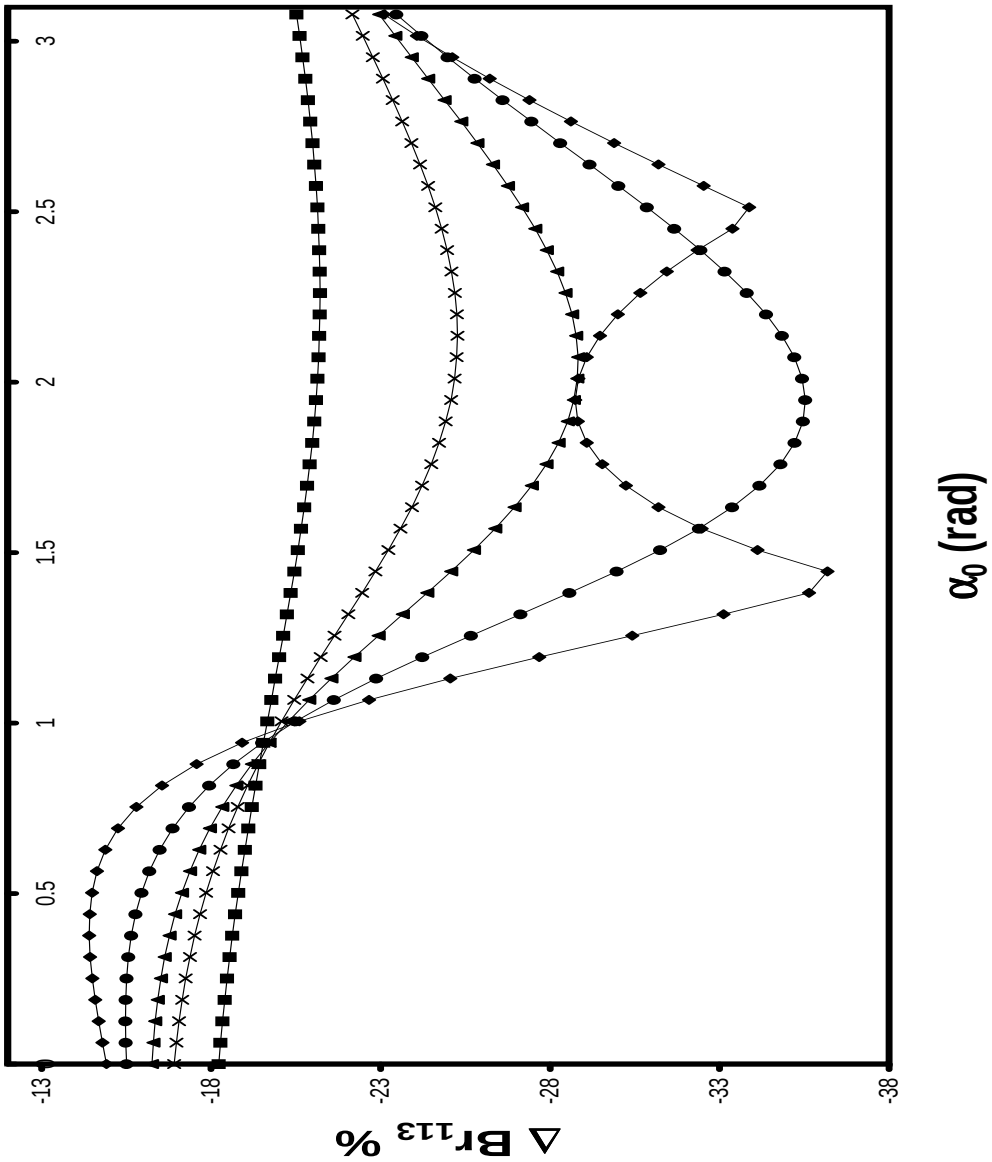

Figure 8: α_0 dependence of $\Delta Br_1 \to \chi_1^0\chi_3^0$. The curves in descending order of the absolute value at $\alpha_0 = 0.0$ (rad) correspond to $|A_0| = 100$, 250, 350, 500 and 650 GeV. The input is $\tan\beta = 30$, $m_{1/2} = 150$ GeV, $m_0 = 500$ GeV, $\xi_1 = 0.5$ (rad), $\xi_2 = 0.6$ (rad), $\xi_3 = 0.7$ (rad) and $\theta_\mu = 1.0$ (rad).

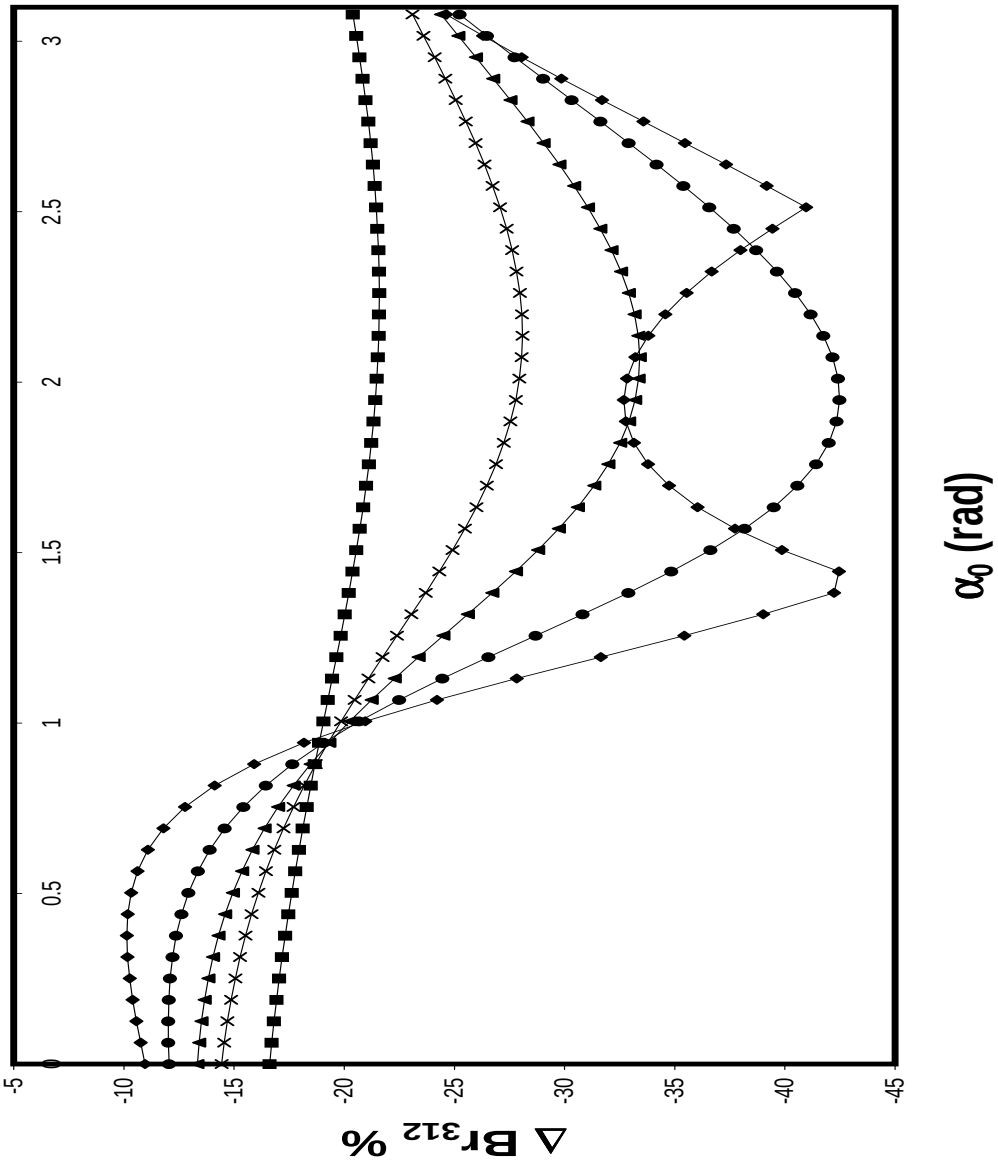

Figure 9: α_0 dependence of $\Delta Br_3 \to \chi_1^0\chi_2^0$. The curves in descending order of the absolute value at $\theta_\mu = 0.0$ (rad) correspond to $|A_0| = 100$, 250, 350, 500 and 650 GeV. The input is $\tan\beta = 30$, $m_{1/2} = 150$ GeV, $m_0 = 500$ GeV, $\xi_1 = 0.5$ (rad), $\xi_2 = 0.6$ (rad), $\xi_3 = 0.7$ (rad) and $\theta_\mu = 1.0$ (rad).

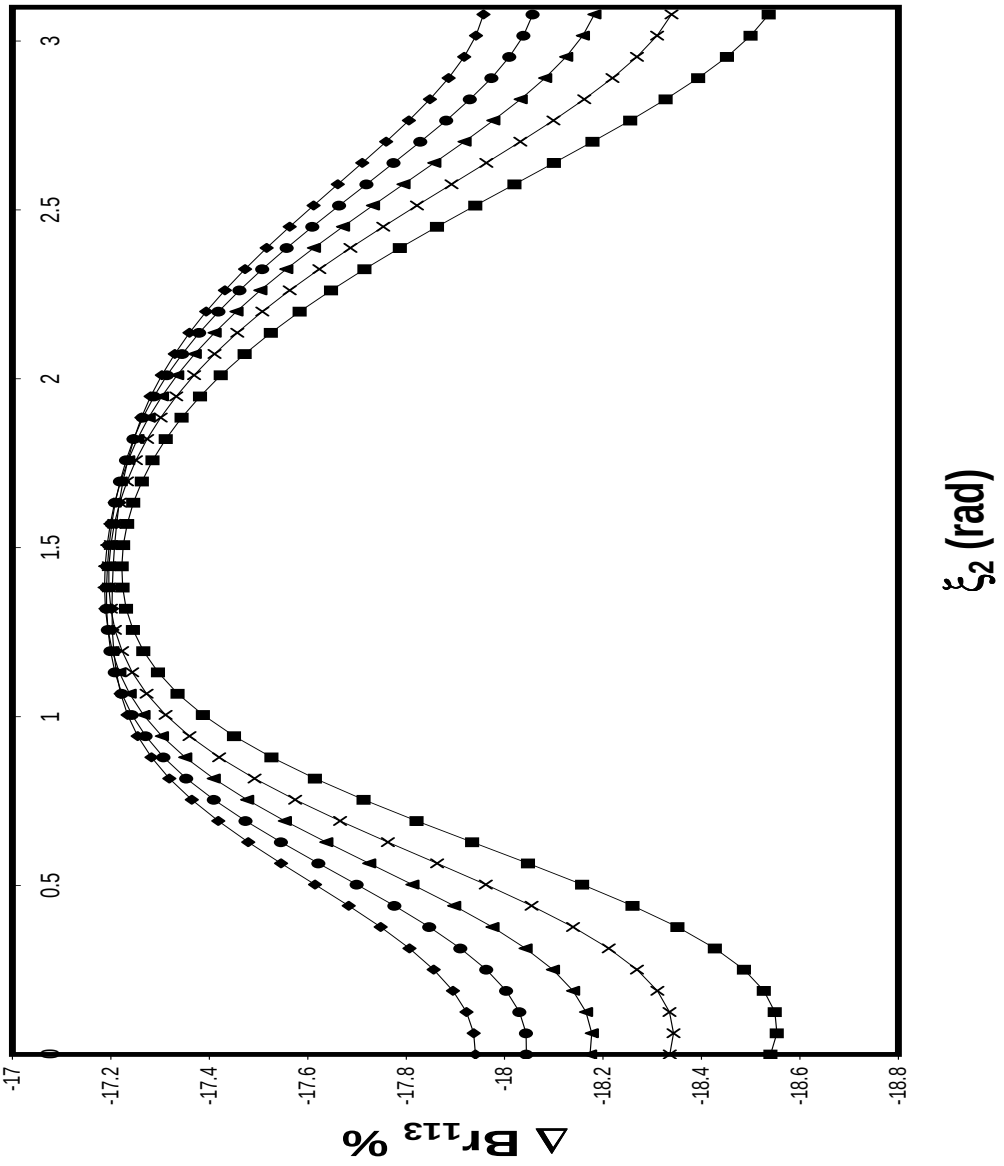

Figure 10: ξ_2 dependence of $\Delta Br_1 \to \chi_1^0\chi_3^0$. The curves in descending order of the absolute value at $\xi_2 = 0.0$ (rad) correspond to $m_0 = 650$, 700, 750, 800 and 850 GeV. The input is $\tan\beta = 20$, $m_{1/2} = 200$ GeV, $|A_0| = 350$ GeV, $\xi_1 = 0.4$ (rad), $\xi_3 = 0.6$ (rad), $\alpha_0 = 0.8$ (rad) and $\theta_\mu = 1.0$ (rad).

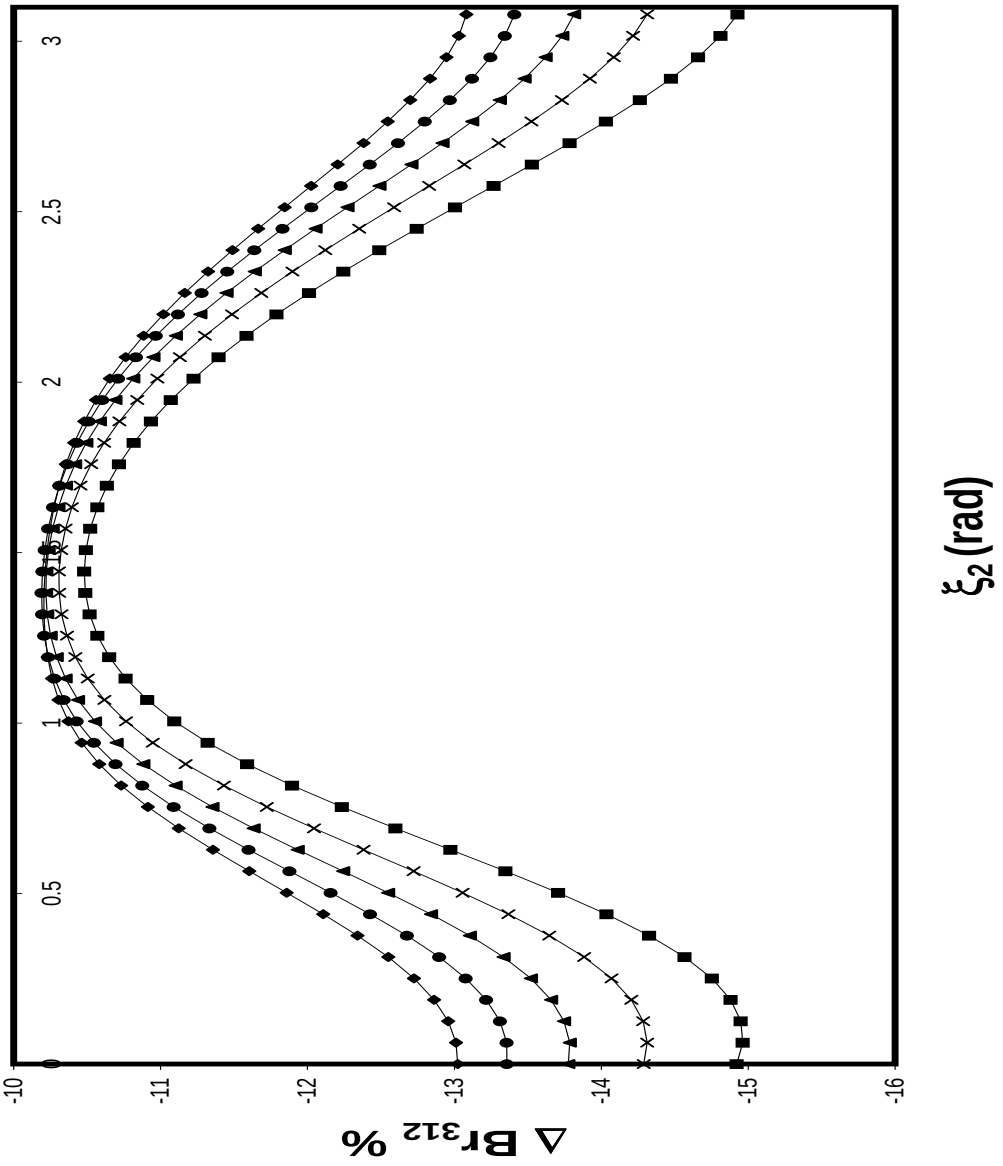

Figure 11: ξ_2 dependence of $\Delta Br_3 \to \chi_1^0\chi_2^0$. The curves in descending order of the absolute value at $\xi_2 = 0.0$ (rad) correspond to $m_0 = 650$, 700, 750, 800 and 850 GeV. The input is $\tan\beta = 20$, $m_{1/2} = 200$ GeV, $|A_0 = 350$ GeV, $\xi_1 = 0.4$ (rad), $\xi_3 = 0.6$ (rad), $\alpha_0 = 0.8$ (rad) and $\theta_\mu = 1.0$ (rad).